



Rifampicin-Carbohydrate Spray-Dried Nanocomposite: A Futuristic Multiparticulate Platform For Pulmonary Delivery

This article was published in the following Dove Press journal:
International Journal of Nanomedicine

Mohammed M Mehanna ^{1,2}
Salma M Mohyeldin ¹
Nazik A Elgindy¹

¹Department of Industrial Pharmacy,
Faculty of Pharmacy, Alexandria
University, Alexandria, Egypt;

²Department of Pharmaceutical
Technology, Faculty of Pharmacy, Beirut
Arab University, Beirut, Lebanon

Purpose: Rifampicin, a first-line anti-tuberculosis drug, was loaded into a carbohydrate-based spray-dried nanocomposite with the aim to design a dry powder inhalation formulation. This strategy can enable efficient distribution of rifampicin within the lungs, localizing its action, enhancing its bioavailability and reducing its systemic exposure consequently side effects.

Methods: The respirable nanocomposite was developed utilizing spray drying of rifampicin nanosuspension employing a combination of mannitol, maltodextrin and leucine as micro-particles matrix formers. Detailed physicochemical characterization and in-vitro inhalation properties of the nanocomposite particles were investigated. Compatibility studies were carried out using differential scanning calorimetry and Infrared spectroscopy techniques. Moreover, pulmonary in-vitro cytotoxicity on alveolar basal epithelial cells was performed and evaluated.

Results: Nanocomposite-based rifampicin-loaded dry inhalable powder containing maltodextrin, mannitol and leucine at a ratio of 2:1:1 was successfully formulated. Rifampicin loading efficiency into the carbohydrate nanocomposite was in the range of 89.3% to 99.2% w/w with a suitable particle size (3.47–6.80 μm) and unimodal size distribution. Inhalation efficiency of the spray-dried nanosuspension was significantly improved after transforming into an inhalable carbohydrate composite. Specifically, mannitol-based powder had higher respirable fraction (49.91%) relative to the corresponding formulation of maltodextrin. Additionally, IC_{50} value of rifampicin nanocomposite was statistically significantly higher than that of free drug thus providing superior safety profile on lung tissues.

Conclusion: The obtained results suggested that spray drying of rifampicin nanosuspension utilizing carbohydrates as matrix formers can enhance drug inhalation performance and reduce cellular toxicity. Thus, representing an effective safer pulmonary delivery of anti-tuberculosis drugs.

Keywords: carbohydrate, inhalation, nanocomposite, rifampicin, tuberculosis

Introduction

Patients with respiratory disorders are usually administered their medications via inhalation.¹ Pulmonary drug delivery offers several merits including its ability to attend higher drug levels at the site of its action, the lung, without the induction of systemic side effects.² Moreover, drugs are not subjected to pre-systemic metabolism unlike oral delivery. In addition, local direct delivery of the drug into the airways is capable of creating fast onset of action with high therapeutic ratio.³

Correspondence: Mohammed M Mehanna
Department of Pharmaceutical Technology,
Faculty of Pharmacy, Beirut Arab University,
P.O.Box 11 - 50 - 20 Riad El Solh, Beirut
11072809, Lebanon
Tel +961 71 708661
Email mmhanna@bau.edu.lb

However, the airway geometry of the lungs poses a challenge for delivery into the alveoli.¹

Tuberculosis (TB) is one of the lethal respiratory infections, which was believed to be extinct but currently more than 30% of the world populations are afflicted with the disease.⁴ TB is the second leading cause of death that comes next HIV infection and according to WHO guideline 2011 reports, 9 million were diagnosed TB with 1.4 million mortality. Most of these cases occurred in Asia and Africa.⁵ The probability of tuberculosis infection increases in immunosuppressive patients, which is mainly due to AIDS.⁶ The most common causative microorganism of TB is *Mycobacterium tuberculosis* among other Mycobacteria strains where 80% of infections affecting the lung and known as pulmonary TB while the extra-pulmonary infections may affect any organ of the body.⁷ Both the primary pulmonary and the secondary extra-pulmonary infections are transmitted through inhalation of *Mycobacterium tuberculosis* bacilli. Obstacles for the ultimate TB curative treatment are the prolong the period of time required for the therapy and the emerging of resistant strains which become more pronounced in immunosuppressive cases.⁸ The treatment of TB infection involves the use of first-line medications, which are isoniazid, rifampicin (RIF), pyrazinamide and ethambutol for 6 months.⁹ In order to target the alveolar macrophages, which are TB infection cellular reservoir, and to control TB respiratory system manifestations, local drug delivery to the lungs by inhalation has been recognized as one of the most attractive routes while reducing systemic adverse effects.⁴ For details concerning the various respirable nanocarriers utilized for TB treatment, our research group has published a review.¹⁰

Microparticles and nanoparticles are utilized as a vehicle for pulmonary drug delivery, but nanoparticles are more promising carrier system. The superiority of nanoparticles is not only due to their smaller size and larger surface area to volume ratios but extends to its higher drug loading capacity, smaller amount of polymer used during its fabrication, better permeability, increased cellular uptake, and longer lung retention and mucus penetration.² In addition, nanoparticles formulation shows an improved drug dissolution property where decreasing the particle size increases the solubility and intracellular drug delivery potential. Moreover, on the cellular level, particles with small sizes are better internalized.^{11,12} Despite these beneficial characteristics of the nanoparticles, delivery of individual particles to the airways is tricky, as their small sizes (<1 μ m) increase their probability of exhalation before

deposition¹³ and their high interparticulate forces which induce uncontrolled aggregation and prevent de-aggregation upon aerosolization under the normal airflow rates in passive dry powder inhalers.¹⁴ Therefore, to optimize the nanoparticles deliver by inhalation, their transformation into micro-scale nanocomposite structures with aerodynamic diameter between 1 and 5 μ m should be performed.¹⁵

Nanocomposite particles are made of drug-loaded nanoparticles and excipients. The excipient function is to form a micro-size matrix where the nanoparticles embed, of which the 3 μ m particle is the most effective to deposit deeply into the lung.¹⁶ Upon the nanocomposite microparticle deposition, it is exposed to the humid environment of the lung and its lining fluid that induce matrix dissolution and decomposition into primary drug-loaded nanoparticles on the surface layer of alveoli.¹⁷ Nanoparticles are able to escape from mucociliary clearance and recognition of alveolar macrophages, therefore, drug-loaded nanoparticles will immigrate towards the epithelial cells where uptake occurred.¹⁸ Yang et al formulated calcitonin-adsorbed polylactic co-glycolic acid (PLGA)-based nanospheres, which was loaded into lactose forming nanocomposites. The prepared nanocomposite particles had efficient lung deposition with a rapid drug release.¹⁹ Hybrid nanoparticles composed of PLGA and soybean lecithin as polymeric and lipid components, respectively, were prepared then transformed into inhalable micro-scale nanocomposites by a novel technique based on electrostatically driven adsorption of nanoparticles onto chitosan particles.¹⁵

Based on the aforementioned information, the current study had investigated the preparation of respirable spray-dried rifampicin nanocomposites (SD-RIF NCs) as a new multiparticulate platform for anti-TB pulmonary delivery to be used as dry powder inhaler (DPI). Spray drying technique was chosen to develop stable re-dispersible solidified nanocomposites for pulmonary delivery of rifampicin. Combination of different inhalable matrix formers, namely, mannitol, maltodextrin, and leucine were evaluated during the spray drying technique. Full in-vitro appraisal of SD-RIF NCs was carried out, including particle size, particle distribution index (PdI), surface charge, drug content and morphological elucidation. Differential scanning calorimetry and infrared spectroscopy techniques were used to study the compatibility between excipients and the drug. The flow properties of the SD-RIF NCs were assessed indirectly in terms of repose angle, Carr's index and Hausner ratio. In-vitro aerosol performance of SD-RIF

NCs was studied using a twin stage liquid impinger. In addition, an in-vitro cytotoxicity study on alveolar basal epithelial cells (A549 cells) was performed to assess the cyto-safety of SD-RIF NCs.

Materials And Methods

Materials

Rifampicin was obtained as a gift sample from Medical Union Pharmaceuticals Company, Egypt. Poloxamer 407, maltodextrin and 3-(4,5-dimethylthiazol-2-yl)-2,5-diphenyltetrazolium bromide (MTT) were obtained from Sigma Aldrich, St. Louis, USA. Leucine was supplied from Fluka, Switzerland. Polyvinyl alcohol (PVA MW 194) was purchased from Adwic, El-Nasr Pharmaceutical Co., Egypt. All organic solvents (methanol and propylene glycol) were of analytical grade and purchased from El-Nasr Pharmaceutical Co., Egypt. Mannitol was purchased from Oxford Lab., Mumbai, India. Lung epithelial cancer cell line A549 was obtained from the American Type Culture Collection, ATCC, USA.

Preparation Of Spray-Dried RIF Nanocomposites (SD-RIF NCs)

Rifampicin nanosuspension was prepared by antisolvent precipitation–ultrasonication technique which was optimized by our group.²⁰ Briefly, RIF (100 mg) was dissolved in methanol and was added into an aqueous solution containing 0.4% w/v of PVA (1:15 v/v, respectively) under continuous sonication at 25°C. Ultrasonication was maintained at room temperature for 30 mins until a homogeneous nanosuspension is obtained.

In order to construct respirable nanocomposites, the prepared nanosuspension was spray-dried using Buchi B-290 mini-spray dryer (Flawil, Switzerland) in the presence of different carrier systems which were either

mannitol or maltodextrin in combination with leucine. The carrier concentrations used are displayed in Table 1. Carriers were added into the RIF NS immediately after preparation under constant stirring until their complete dissolution. Then, the dispersion was spray-dried with a mini-spray dryer apparatus equipped with a high-performance cyclone, two component nozzles, and co-current flow. The spray drying conditions were; inlet temperature of 110°C, 100% aspiration air, 10% pump rate, and 320 L/h airflow rate. The spray-dried powders were collected and stored in a desiccator on CaCl₂ at 25°C for further investigations.

Physicochemical Characterization Of Spray-Dried RIF Nanocomposites Yield Recovered Determination

The yield value of the produced powders was determined as percentage of the original amounts of solids used. The yield was calculated as follows:

$$\% \text{ Yield} = \left[\frac{\text{Mass of spray-dried powder recovered}}{\text{Total mass of solid used in formulation}} \right] \times 100 \quad (1)$$

Determination Of Drug Content

An accurately weighed amount of each batch of spray-dried rifampicin nanocomposite (SD-RIF NC) was completely dissolved in 1:1v/v methanol/water mixture. Then, the resultant solution was filtered through 0.22 μm Millipore syringe filter. The dissolved RIF was determined spectrophotometrically at λ_{max} 477 nm. The drug content was determined as percentage of the theoretical drug amount used in the formulation, calculated by three determinations for each sample.

Table 1 Composition, Yield, And Drug Content Of Spray-Dried Rifampicin Nanocomposites

Formula	Carrier/Nanosuspension (w/w) Ratio			Yield* % w/w	Drug Content* % w/w
	Mannitol	Maltodextrin	Leucine		
F ₁	4	–	–	44.80±3.13	90.4±1.71
F ₂	3	–	1	61.24±2.67	96.3±3.24
F ₃	2	–	2	66.65±3.35	92.6±2.06
F ₄	–	4	–	71.40±1.51	89.3±4.04
F ₅	–	3	1	79.84±2.84	91.3±4.03
F ₆	2	1	1	73.05±3.34	98.3±0.75
F ₇	1	2	1	86.67±2.08	99.2±3.32

Note: *Mean±SD (n=3).

$$\% \text{ Drug content} = \left[\frac{\text{Mass of drug in spray-dried powder}}{\text{Mass of drug used in formulation}} \right] \times 100 \quad (2)$$

Spray-Dried Powder Morphology

The topological and morphological characteristics of SD-RIF NC were investigated through scanning electron microscope (model JEM-100S, Joel, Japan). The dried powder samples were fixed on aluminum stubs using a double-sided adhesive tape and coated with gold at 2 mA for 3 mins through a sputter-coater under an air atmosphere. A scanning electron microscope with a secondary electron detector was used to obtain photoelectromicroscopical images at an accelerating voltage of 10 kV.

Particle Size Measurements

Particle size and size distribution of the spray-dried powders were determined by laser diffraction analyzer (Cilas L100, model 1064 liquid, Quantachrom, Orleans, France). For this purpose, each of the SD sample was dispersed in isopropanol and sonicated for 1 min before measurement. The suspension was added into the sample cell containing the same dispersion medium. The analysis was repeated in triplicate. The data obtained were expressed in terms of volume median diameter ($D_{V50\%}$). The polydispersity of the powders was expressed by the span index, which was calculated as follows:²⁰

$$\text{Span index} = \frac{D_{(v,90)} - D_{(v,10)}}{D_{(v,50)}} \quad (3)$$

where $D_{(v,10)}$, $D_{(v,50)}$, and $D_{(v,90)}$ are the equivalent volume diameters at 10%, 50%, and 90% cumulative volumes, respectively.

Specific Surface Area

The surface area of the nanocomposites was measured using NOVA[®] 1000 surface area analyzer (Quantachrome instruments, Europe). Approximately 50 mg of each formulation was dried at 50°C under vacuum and the volume of sample cell was measured at room temperature. Nitrogen adsorption and desorption measurements were performed using sample and empty reference cells immersed in liquid nitrogen. The average surface area was calculated by BET equation (Brunauer–Emmett–Teller) method.²¹

Particle Size Analysis Of Reconstituted SD-RIF NCs

The freshly prepared SD-RIF NCs were first reconstituted by dispersing in deionized water via vortex mixer for 1 min. The particle size and size distribution of reconstituted

SD-RIF NCs were assessed by dynamic light scattering (DLS) technique using NanoZS/ZEN3600 Zetasizer (Malvern Instruments Ltd., UK) equipped with Malvern PCS software (version 6.2). All DLS measurements were performed under controlled temperature condition at 25 ±0.1°C at 20 s intervals for three repeated determinations. The particle size and size distribution were expressed as z-average and polydispersity index (PdI), respectively. Moreover, re-dispersibility index (RDI) was calculated as follows:¹³

$$\text{RDI} = \left[\frac{z\text{-average}}{z\text{-average}_0} \right] \quad (4)$$

where z-average is the corresponding value of nanosuspension reconstituted from SD-RIF NCs upon rehydration and $z\text{-average}_0$ is the intensity-weighted mean particle diameter of the nanosuspensions prior to spray drying.

Zeta Potential Measurements Of Reconstituted SD-RIF NCs

The electrophoresis mobility of the reconstituted SD-RIF NCs was measured using NanoZS/ZEN3600 Zetasizer (Malvern Instruments Ltd., UK) then zeta potential was calculated using the dispersion technology software provided by Malvern (Malvern Instruments Ltd., UK). Each sample was performed in triplicate.

Spray-Dried Powder Flowability

The flow properties of the SD-RIF NCs were assessed indirectly using a flowability tester (model BEP2, Copley Scientific Ltd., UK) with an angle of repose attachment. Each measurement was performed in triplicate and angle of repose (θ) was calculated.²² Furthermore, SD-powder flowability was evaluated by determining the Carr's index (CI) and Hausner ratio (HR) for each formulation.²³ A pre-weighed quantity of dry powder was poured into a 10 mL graduated measuring cylinder. The apparent volume occupied by the powder was noted as bulk volume (V_b). Then, the measuring cylinder was tapped 1000 times using the tap density tester (Stampfvolumeter STAV 2003; Engelsmann, Ludwigshafen, Germany) until a constant volume was obtained and recorded as the tapped volume (V_t). Each experiment was run in triplicate and results were shown as mean±SD. The bulk (ρ_{bulk}) and tapped (ρ_{tap}) densities of powders were calculated. Moreover, Carr's index (CI) and Hausner ratio (HR) were calculated according to the following equations:²²

$$\% \text{ CI} = \left[\frac{\rho_{\text{tap}} - \rho_{\text{bulk}}}{\rho_{\text{tap}}} \right] \times 100 \quad (5)$$

$$\text{HR} = \frac{\rho_{\text{tap}}}{\rho_{\text{bulk}}} \quad (6)$$

In-Vitro Dissolution Studies

In-vitro dissolution behavior of RIF from the NS was assessed using the USP XXIV dissolution apparatus II. The SD-RIF NCs (equivalent to 50 mg drug) were sprinkled on the surface of 300 mL PBS (pH 7.4) as a dissolution medium at $37 \pm 0.5^\circ\text{C}$. At predetermined time intervals, samples were withdrawn and analyzed for its rifampicin content spectrophotometrically at λ_{max} 474 nm. All runs were performed in triplicate. The dissolution efficiency percentage (%DE) and the mean dissolution time (MDT), as parameters for the extent and rate of dissolution, respectively were calculated according to the following equations:^{13,24}

$$\% \text{ DE} = \left[\frac{\int_0^t y \times dt}{y \times 100 \times t} \right] \times 100 \quad (7)$$

where y is the percentage of drug dissolved.

$$\text{MDT} = \frac{\sum_{i=1}^n t_{\text{mid}} \Delta M}{\sum_{i=1}^n \Delta M} \quad (8)$$

where i is the dissolution sample number, n is the number of dissolution times, t_{mid} is the time at the midpoint between times t_i and t_{i-1} , and ΔM is the amount of drug dissolved (mg) between times t_i and t_{i-1} .

Evaluation Of Aerosolization Performance Of The Nanocomposite

Measurement Of Theoretical Aerodynamic Diameter (d_{ae})

The theoretical d_{ae} of the particles was calculated based on the following equation:²⁵

$$d_{\text{ae}} = d_{0.5} \times \sqrt{\frac{\rho_{\text{tap}}}{\rho}} \quad (9)$$

where $d_{0.5}$ is the median particle size, ρ_{tap} is the powder tapped density (g/cm^3) and ρ is the density of sphere (equal to $1 \text{ g}/\text{cm}^3$).

In-Vitro Aerosol Deposition

Aerodynamic behavior of the SD-RIF NCs was assessed using Aerolizer[®] (Novartis Pharmaceutical UK, England) as an inhaler device connected to the twin stage liquid

impinger, TSI (Copley Scientific Ltd., UK). Volumes of 7 and 30 mL of mixture of methanol and water (1:1 v/v) were introduced into stages 1 and 2, respectively.²⁶ An accurately weighed sample of SD-RIF NCs was filled in a hard gelatin capsule (size 3), placed into the Aerolizer[®] which was attached to the throat of the impinger via the adaptor. The impinger operated at a flow rate of 60 L/min, which was adjusted using an electronic digital flowmeter. The powder deposited on each of the two stages of the impinger was collected and RIF content was quantified spectrophotometrically at λ_{max} 477 nm.

The in-vitro aerosolization properties of the powders were described in terms of emitted dose (ED) and emitted dose fraction (EF) were determined,²⁶ in addition to, the respirable particle fraction (RF) and the effective inhalation index (EI) that were calculated by the following equations:²⁶

$$\text{RF} = \left[\frac{\text{St}_2}{\text{ED}} \right] \times 100 \quad (10)$$

$$\text{EI} = \sqrt{\text{EF} \times \text{St}_2} \quad (11)$$

where St_2 is the amount of powder collected at stage 2 of the twin stage impinger.

Drug-Excipient Compatibility Studies

Differential Scanning Calorimetry (DSC)

Thermal behavior of RIF, mannitol, maltodextrin, leucine, selected SD-RIF NCs, and their physical mixture were assessed using the DSC analysis (Perkin Elmer, USA). An accurately weighed sample of each powder (5 mg) was loaded in a sealed aluminum pan and heated at a rate of $10^\circ\text{C}/\text{min}$ under a nitrogen atmosphere purged at 40 mL/min in the temperature range from 25 to 300°C .

Fourier Transform Infrared (FTIR) Spectroscopy

Fourier transform infrared (FTIR) spectroscopy was employed to detect drug-excipient compatibility or interaction (FTIR spectroscopy, PerkinElmer, USA). Samples were finely ground with infrared grade KBr then pressed into pellets at ambient temperature. FTIR spectra were recorded in transmission over the range of $4000\text{--}400 \text{ cm}^{-1}$ with a resolution of 4 cm^{-1} . Samples assessed encompassed RIF, mannitol, maltodextrin, leucine, selected SD-RIF NCs, and their physical mixture.

X-Ray Diffraction (XRD)

The crystalline structure of prepared samples were examined using wide angle X-ray diffraction, XRD (X'Pert PRO diffractometer, PANalytical, The Netherlands). A copper

radiation source was used as the anode material. The diffraction pattern was performed in a step scan model with a voltage of 40 kV and a current of 30 mA in the range of 4° to 42° using a step size of 0.02 2 θ with a dwell time of 2 s. Samples investigated were RIF, mannitol, maltodextrin, leucine, spray-dried NS, the selected SD-RIF NCs, and their physical mixture.

In-Vitro Cytotoxicity Study

To ensure the safety of the drug delivery system, cytotoxicity of the selected formulations as well as pure RIF was assessed using MTT [3-(4,5-dimethylthiazol-2-yl)-2,5-diphenyltetrazolium bromide] assay on lung epithelial cells.

Cell Culture

The human alveolar basal epithelial cells (A549 cells) were cultured in F-12 Ham supplemented with 10% fetal bovine serum, 1% glutamine, and 100 μ g/mL penicillin/streptomycin antibiotics. The A549 cells were maintained in a humidified air atmosphere (37°C, 95% humidity and 5% CO₂) as previously reported.²⁷

Cytotoxicity Assay

The A549 cells were seeded into a 96-well plate at a density of 1×10^4 cells/well for 24 hrs. Afterwards, the cells were treated with various concentrations of the pure drug as well as the selected SD-RIF NCs and incubated for another 24 hrs. The cell viability after treatment was examined by MTT assay. The percentage of cell viability related to control cells incubated with culture medium only was determined. The MTT assay for each concentration was performed in triplicate. The 50% cytotoxic concentration (IC₅₀) was estimated graphically.

Storage Stability

A short-term storage was performed to assess the physical stability of the SD-RIF NCs (F₇) which was packed in capped amber glass vials and stored in a desiccator on CaCl₂ at 25°C for a period of 6 months. The percentage of drug content, particle size, PdI, and ZP of the sample were monitored on day zero and followed 6 months. Furthermore, the tapped density and the particle size of the stored formula (Dv_{50%}) were measured in order to calculate the theoretical aerodynamic diameter. The in-vitro dissolution behavior of stored nanocomposites was also evaluated.

Statistical Analysis

Results were expressed as the mean of three independent experiments \pm standard deviation. Statistical data analysis was carried out using the one-way analysis of variance test (ANOVA). Difference was considered statistically significant at a level of *p*-value <0.05.

Results And Discussion

Inhalable therapeutic nanoparticle as a drug delivery vehicle represents a potential area of nanotechnology applications.²⁸ Although its small sizes hinder their transport into deep alveoli and lung tissues. Thus, the development of an efficient carrier system turned to be a prerequisite for nanoparticles proper lung disposition, which is still challenging the researchers. The main concerns about the carrier system selection beside their pulmonary safety are; its ability to maintain drug stability, its smooth handling protocol during processing, its capability to form particles with appropriate aerodynamic properties for ultimate lung deposition, and its ability to provide free flowing powder which aids in drug dispersion from inhalers.^{29,30} Thereby, the nanoparticles loading into micro-sized particles are captivating. Recently, microspheres-encapsulating nanoparticles using the spray drying technique were reported.³⁰⁻³²

Spray drying is a friendly technology that converts a fluid feed into a dried particulate in a single step. It receives great attention in the field of pharmaceutical production as it produces dry powder with specific characteristics, rapid process, can be manipulated to suit heat-sensitive drugs and can be scaled-up easily. As previously documented, for the production of inhalable dry powders, spray drying is a commonly used technique in pharmaceutical industry.³³ The wide acceptance of spray drying as particle engineering technique for the design of DPI formulations is related to the ability to control and tailor the process parameters in order to optimize the particle properties, namely surface morphology, size, size distribution, flowability, and moisture content.³⁴

In this attempt, respirable spray-dried rifampicin nanocomposites having a theoretical aerodynamic diameter between 1 and 5 μ m were successfully prepared by a two-step process. The first step involved the formation of RIF nanocrystals using the antisolvent precipitation-ultrasonication method. The second step was the transformation of these nanocrystals into micro-scale nanocomposite

structures using a mini-spray dryer in the presence of matrix formers.

Matrix former carbohydrates, namely; sugar alcohol (mannitol) or polysaccharide (maltodextrin), were selected based on their reported capability of being drying protectants during water removal phase and of shaping the nanocomposite through controlling particle/particle interactions.^{13,26} The amino acid L-leucine was provided to be an aerosolization enhancer through forming a shell on the particles surface preventing their fusion.¹³ Moreover, it was employed due to its ability to improve powder dispersibility as previously reported.^{26,35}

As shown in Table 1, several spray-dried formulations (varying the ratio between the matrix formers, nanosuspension, and the amino acid) were investigated aiming at developing a powder formulation with the highest emitted dose and fine particle fraction.

Physicochemical Characterization Of Spray-Dried Rifampicin Nanocomposites Percentage Of Yield

The yield values of the spray-dried powders varied between 30.65% and 86.67% w/w during spray drying processing as illustrated in Table 1. In spite of the use of a high-performance cyclone, the yield values of NS in the absence of any matrix former did not exceed 30.65% w/w. The use of either mannitol or maltodextrin was significantly accompanied by yield increase to 44.80 (F₁) and 71.4 (F₄) % w/w, respectively (p -value <0.05). The usage of the high molecular weight maltodextrin at the same ratio significantly raised the yield recovered relative to that of the low molecular weight mannitol (p -value=0.0002). The effect of mannitol on the yield is similar to that reported by Kumar et al, which is correlated to the glass transition temperature (T_g) of carbohydrates where sugars with low T_g, as mannitol, generally stick to the spray dryer chamber due to its rubbery state.³⁶ The superiority of maltodextrin that had been reported is due to its high glass transition temperature even at high relative humidity.^{26,37} Polysaccharides had also been recently described to preserve protein stability owing to its high molecular weights.^{36,38}

With regard to Table 1, inclusion of L-leucine in mannitol-based (F₂) or maltodextrin-based formula (F₅) resulted in improving spray-dried yield significantly, 61.24% and 79.84% w/w, respectively (p -value <0.05). It may be probably due to the slight hydrophobic nature of leucine which provided a water repellent effect, reducing moisture uptake,

decreasing powder agglomeration and stickiness and improving its flow properties.²⁶ The same finding was reported by Moghaddam et al,³⁹ where clarithromycin-loaded PLGA nanoparticles were co-sprayed with either mannitol or lactose in the presence of leucine as a third component. The leucine incorporation in the formula resulted in a significant increase of yield from 22.50% to 37.90% w/w and from 32.87% to 46.50% w/w in case of mannitol and lactose, respectively. However, doubling the leucine concentration (F₃) insignificantly increased the obtained yield corresponding to that of F₂ (p -value=0.0935). A comparable result was observed by Osman et al,⁴⁰ where the addition of leucine caused a significant increase in the yield of the spray-dried DNase I microparticles depending on its concentration, reaching a maximum of about 40% increase in a formulation containing 30% w/w of leucine. Further increase in leucine concentration to 60% w/w did not affect the yield parameter.²⁵

Combination of maltodextrin and mannitol in both F₆ and F₇ lead to an increase in the yield compared to F₂ and F₅, respectively (p -value <0.05). This observation was in accordance with previous literature demonstrating that the presence of dextran (polysaccharide) with a disaccharide was able to suppress particles shrinkage and collapse of due to T_g modulation.²⁶ Similarly, Kumar et al³⁶ used a mixture of a low molecular weight and a high molecular weight sugars to improve the spray drying yield. On the opposite, mannitol combined with lactose in another study dramatically decreased the powder yield. This was attributed to the “sticky point” where interparticulate cohesion forces sharply increased, inducing adhesion of the spray-dried powders to the drying chamber and the collecting cyclone.³⁹

Rifampicin Content In SD-RIF NCs

An efficient active pharmaceutical ingredient distribution within the particles is a crucial parameter for the administered dose uniformity. RIF content for the different formulations is summarized in Table 1. The measured values of SD-RIF NCs were very close to their expected values, with percentage of drug content ranging from 89.3% to 99.2% w/w. Thus, the active ingredient seemed to be uniformly distributed in the different SD-RIF NCs powders.

Indeed, depending on the excipient used and their ratios, different values of RIF content were observed as depicted in Table 1. Without matrix former, free nanosuspension (NS) showed the lowest RIF content after spray drying. This significant loss of RIF may be related to its

poor aqueous wettability that induced solid phase separation and caused adhesion of RIF to the glass walls of the drying chamber. Furthermore, in the absence of carrier, the nanocrystals possessed a greater probability of being eroded or detached during the spray drying procedure due to their high specific surface areas.²⁵ Once detached, these small nanocrystals could be carried out by the airflow and lost in the filter collector. The fraction that was removed by the airflow was the reason for the loss of the active ingredient. The same phenomena were observed by Pomázi et al,⁴¹ where the percentage of meloxicam content in the spray-dried microcomposites was significantly decreased from 48.95% to 27.74% w/w after drying without using any additives.

In the presence of matrix formers either mannitol (F₁) or maltodextrin (F₄), the real and theoretical RIF contents were closer to each other. However, the addition of leucine caused a non-significant increase in drug content from 90.4% (F₁) to 96.3% w/w (F₂) and from 89.3% (F₄) to 91.3% w/w (F₅) (*p*-value=0.109 and 0.576, respectively). Similarly, leucine with different concentrations did not significantly enhance the percentage of DNase I content in the spray-dried microparticles, ranging from 63%±3.8% to 71%±4.8% w/w in formulations without and with leucine, respectively.⁴⁰ Moreover, the matrix formers combinations in both F₆ and F₇ improved the percentage of RIF content but with non-significant values relative to that of F₂ and F₅, respectively (*p*-value >0.05).

Morphological Characterization Of Spray-Dried RIF Nanocomposites

In the current study, morphology of spray-dried RIF nanocomposite powders was evaluated by SEM analysis. The photomicrographs of raw rifampicin and some selected spray-dried RIF nanocomposites powders (NS, F₁, F₂, F₄, F₅ and F₇) are demonstrated in Figure 1.

The scanning electromicrograph of raw rifampicin (Figure 1A) revealed the presence of large crystals aggregated together with a particle size that is too large for inhalation. Following the spray drying of the RIF nanosuspension (NS) alone without the usage of any matrix formers, aggregated and agglomerated spherical particles were observed (Figure 1B). Since the drying adjuvants are expected to protect the nanocrystals against particle/particle interactions, thus preventing their aggregation.

The inclusion of different water-soluble matrix formers in the external phase changed the particle morphology by uniformly spreading on the particles surface giving them a

different appearance. Mannitol-loaded RIF nanocomposites (F₁) showed separated spherical particles with moderately corrugated surface (Figure 1C). During spray drying process, the surface layers collapsed when the vapor pressure is high, resulting in the formation of spherical particles with wrinkled surface. When mannitol was present in a sufficient amount to form a complete surface layer, thus it would inhibit the passage of the water vapor formed as result of high temperature and then the surface layer was expanded like a balloon. After complete water evaporation, the surface layer would collapse resulting in the wrinkled structure.⁴⁰ Contrastingly, by using maltodextrin as a matrix former (F₄), non-aggregating spherical particles with a smooth surface were formed (Figure 1D). It was clear that the surface layers formed during droplets drying in the presence of mannitol (F₁) were weaker than that formed in the presence of maltodextrin (F₄) and hence the particles collapsed upon water evaporation.²⁶

Moreover, SEM images of particles surfaces of powder formulations containing leucine (F₂ and F₅) revealed an increased surface rugosity (Figure 1E and F). By virtue of leucine hydrophobicity and surface activity, it had a good tendency to accumulate at the interfacial area of the droplets, reducing their particle cohesiveness. The mentioned results are in a close accordance with previous reports on the surface properties of L-leucine during spray drying process.^{26,42-44}

By combining the high molecular weight maltodextrin with the low molecular weight mannitol in either F₆ or F₇, spherical particles with less corrugated surface and size varying from 1 to 4 μm were obtained (Figure 1G and H). The use of different ratios between mannitol and maltodextrin showed the same effect on the surface morphology of SD-RIF nanocomposites powders. The presence of maltodextrin with mannitol was able to suppress the shrinkage and collapse of particles due to the change in their glass transition (T_g). Furthermore, the formation of a thicker layer on the surface of nanocomposite particles prevented their collapse during the spray drying process.

Particle Size Of Spray-Dried RIF Nanocomposites

The dispersion and deposition pattern of the dry powder inhalation formula is mainly controlled by its particle size, together with its density, which are the key factors for the success of the inhalable formulation.⁴⁵ Particle size of spray-dried powders was determined using a laser light-scattering technique. In the preliminary study, isopropyl alcohol was chosen as a suspending medium among the

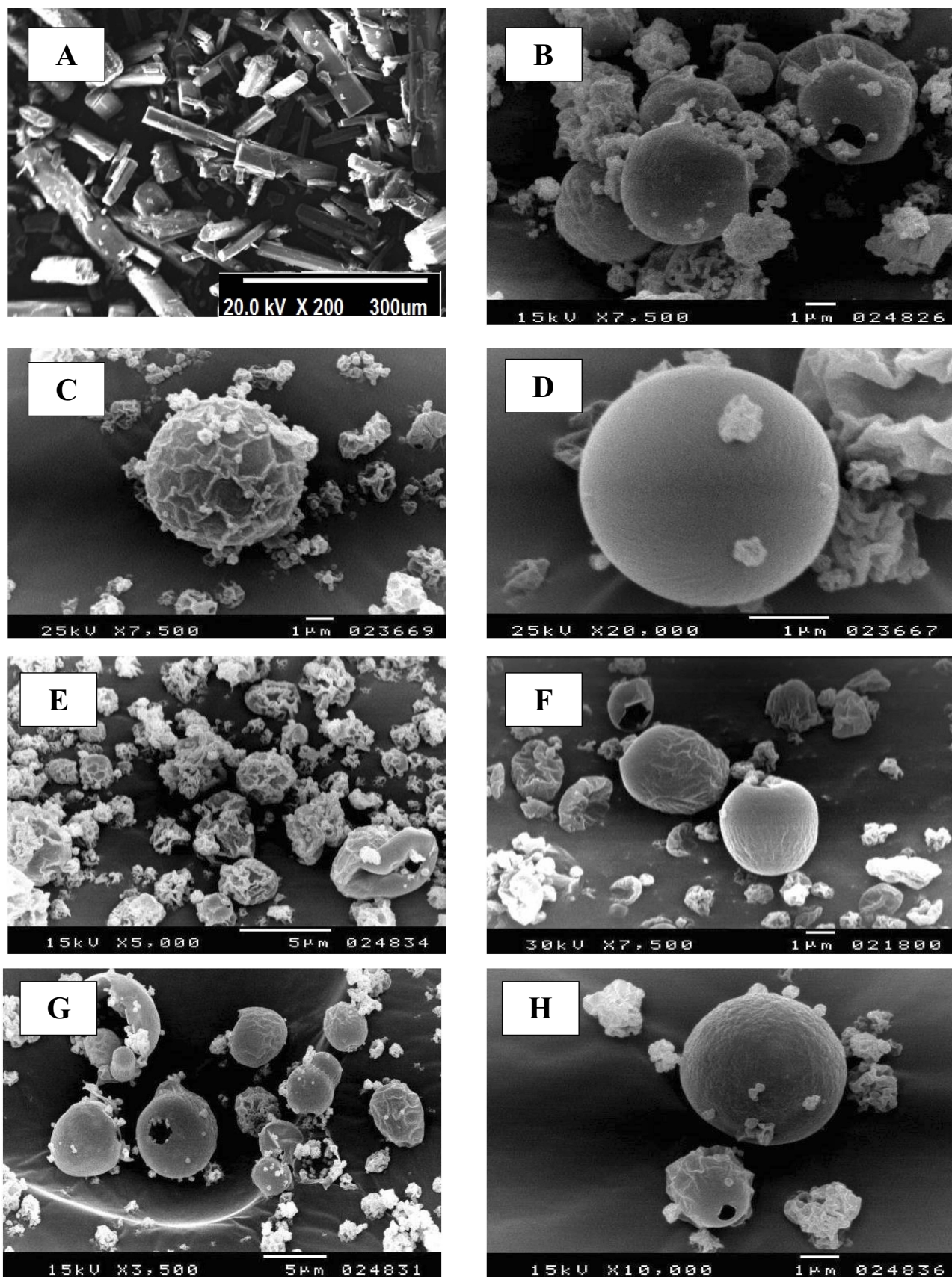


Figure 1 Scanning electron microscope (SEM) micrograph of raw rifampicin (A), spray-dried nanosuspension (B) and selected spray-dried rifampicin nanocomposites powders F₁ (C), F₄ (D), F₂ (E), F₅ (F), F₇ (G) and F₇ at higher magnification (H).

other solvents. For all formulae, the particle size distribution curves showed a unimodal distribution with no evidence of existence of various size populations. Spray-dried RIF NS powder alone without any matrix formers exhibited a large particle size ($Dv_{50}=22.9\pm 3.20\ \mu\text{m}$), revealing the presence of large agglomerates and aggregates as early proved in the SEM micrograph. In contrast, the size of spray-dried nanocomposites powder (Dv_{50}) was significantly smaller ranging from 3.47 to 6.80 μm (p -value <0.005) indicating suitability for lung deposition. The low span values proved a narrow particle size distribution as depicted in Table 2.

The inclusion of hydrophilic matrix former either mannitol (F_1) or maltodextrin (F_4) to RIF nanosuspension resulted in a significant reduction in particle mean diameter to 5.12 ± 0.13 and $6.25\pm 0.31\ \mu\text{m}$, respectively. The addition of matrix former proved to minimize the inter-nanoparticle fusion attributed to the closer interaction between nanoparticles during the spray drying operation. Similarly, Malamatarı et al¹³ reported that the indomethacin nanoparticles agglomerates prepared without matrix formers have significantly higher median diameter ($Dv_{50\%}$) compared to that containing matrix formers. The combination of maltodextrin and mannitol in both F_6 and F_7 revealed non-significant difference in the particle diameter in comparison to F_2 (p -value=0.112) and F_5 , (p -value=0.405), respectively.

As shown in Table 2, F_1 containing mannitol as a matrix former showed a significant smaller mean particle diameter ($Dv_{50\%}$) relative to the F_4 containing maltodextrin (p -value=0.004), which might be attributed due to their surface energy difference. It was reported that the surface energy of the high molecular weight maltodextrin was greater than that of the low molecular weight sugars.⁴⁶ Thus, maltodextrin formulation (F_4) showed aggregation

during laser diffraction measurement, as the shear forces exerted on the particles did not overcome the surface energy of maltodextrin required to break the particles adhesion.

A significant decrease in the particle diameter ($Dv_{50\%}$) was observed as a result of incorporation of leucine in the aerosol formulations (F_2 and F_5) compared to the corresponding formulations F_1 and F_4 , respectively (p -value=0.0028 and 0.0056, respectively). This effect was in line with a previous study where addition of leucine to mannitol before spray drying of chitosan nanoparticles led to a decrease in particle size of the spray-dried products from 10.9 to 6.7 μm .⁴⁷ As a result of leucine hydrophobicity, it tends to accumulate at the air-liquid interface, thus effectively reducing the size of the droplets produced at the spray dryer nozzle, explaining the observed particle size reduction.⁴⁴ However, further increase in leucine concentration (F_3) resulted in increased particle diameter ($Dv_{50\%}$) to $6.80\pm 0.71\ \mu\text{m}$. This may be due to the accumulation of solid L-leucine mainly on the droplet surface leading to the formation of thicker solid shells, resulting in the formation of powders having a larger diameter.

Specific Surface Area Of Spray-Dried RIF Nanocomposites

In order to study the effect of the spray drying technique on the powder properties, specific surface area of SD-RIF NCs was measured. The results (Table 2) showed different values of surface area in the range of 1.343 (F_4) to 3.997 m^2/g (F_3). Mannitol-based SD NC (F_1) revealed a higher surface area value (2.169 m^2/g) relative to the corresponding formula containing maltodextrin (F_4 , 1.343 m^2/g). Furthermore, the inclusion of leucine in the formulations (F_2 , F_3 , and F_5) led to an increase in the surface area value (3.105, 3.997, and 2.942 m^2/g , respectively).

Table 2 Particle Size Distribution And Surface Area Of Spray-Dried Rifampicin Nanocomposites

Formula	$Dv_{(10\%)}\ (\mu\text{m})$	$Dv_{(50\%)}\ (\mu\text{m})$	$Dv_{(90\%)}\ (\mu\text{m})$	Span Index	Surface Area (m^2/g)
NS	11.3 \pm 2.95	22.9 \pm 3.20	41.12 \pm 2.09	1.30 \pm 0.201	–
F_1	1.22 \pm 0.12	5.12 \pm 0.13	10.53 \pm 1.42	1.81 \pm 0.230	2.169
F_2	1.83 \pm 0.12	3.47 \pm 0.42	09.73 \pm 1.56	2.28 \pm 0.209	3.105
F_3	2.35 \pm 0.17	6.80 \pm 0.71	13.00 \pm 0.79	1.57 \pm 0.071	3.997
F_4	1.51 \pm 0.11	6.25 \pm 0.31	13.68 \pm 1.02	1.95 \pm 0.104	1.343
F_5	1.21 \pm 0.07	4.35 \pm 0.52	11.61 \pm 1.44	2.39 \pm 0.058	2.942
F_6	1.95 \pm 0.35	4.77 \pm 1.03	10.42 \pm 1.18	1.80 \pm 0.206	3.089
F_7	1.58 \pm 0.23	3.85 \pm 0.77	09.06 \pm 0.47	1.94 \pm 0.512	3.065

Note: Data are presented as mean \pm SD (n=3).

The combination of mannitol and maltodextrin in the SD NC (F₆ and F₇) revealed no difference in the surface area.

An explanation of these phenomena could be withdrawn from the SEM micrographs of SD-nanocomposites (Figure 1). The corrugated and wrinkled surface of F₁ particles led to an increase in the surface area in comparison to the smooth surface of F₄ nanocomposites. The addition of leucine resulted in highly corrugated surface, thus leading to a further increase in the surface area values. A similar observation was reported by Chew and Chan,⁴⁸ who concluded that a non-porous corrugated particle had a larger surface area compared to the smooth spherical ones. Thus, the surface roughness and the irregularity of SD NCs should be taken into consideration as it has a direct effect on the spray-dried particles physical properties.

Particle Size And Zeta Potential Of Reconstituted SD-RIF NCs

Regarding the redispersibility and reconstitutibility properties, for the spray-dried nanocomposites, it is desirable to be rapidly dispersed to yield the primary nanoparticles upon contact with pulmonary secretions. Table 3, based on the redispersibility index (RDI) data, all SD-nanocomposites formulation was able to liberate nanoparticles upon their aqueous reconstitution with RDI values in the range of 1.1 (F₂) to 4.7 (NS).

Spray-dried nanosuspension yield nanoparticles with a higher z-average value around 473 nm relative to the original nanosuspension (101.7 nm). This might be due to the thermal stress caused by the drying phase which led to irreversible nanoparticles aggregation, probably due to steric stabilization inactivation which was provided by the polymeric stabilizer in the liquid form.¹³ More specifically, removal of water molecules in between the nanocrystals

might induce entanglement of the stabilizer chains or stabilizer fusion, which could further lead to irreversible particle agglomeration.⁴⁹ Another possible explanation for NS inability to re-disperse completely is that stabilizer, PVA, which was coating the nanocrystals surface re-crystallized during spray drying thus compromised its ability to prevent aggregation.¹³ Similar observation was previously reported where severe aggregation of the nanoparticles occurred after the spray drying of itraconazole nanosuspension in the absence of matrix formers.²⁵ Otherwise, nanocrystals aggregation was decreased in the presence of different matrix formers (F₁-F₇), as evidenced by lower RDI values, ranging from 1.1 (F₁) to 2.7 (F₅).

The influence of carbohydrates on the aggregation behavior of nanocrystalline suspensions of the poorly soluble drug RIF during spray drying process was investigated. Mannitol-based powder (F₁) was easily dispersed in deionized water giving a nanosuspension with smaller nanocrystals size (111.2 nm) compared to maltodextrin-based powder (F₄) but with a higher PdI. The recovery of nanocrystals in the sugars solutions could be due to their chemical structure (polyhydroxy compounds), which is able to be adsorbed at the interface and intercalate onto the interfacial film of the nanocrystals decreasing their contacts after reconstitution.²⁶ Similarly, during spray drying of indomethacin nanosuspension, researchers reported an increase in their size in case of maltodextrin compared to smaller molecular weight sugars as a result of their favorable interactions and steric effects.³⁶

The inclusion of leucine in the formulation (F₂ and F₅) had an adverse effect on the particle size of nanocrystals liberated; exhibiting RDI values of 1.2 and 2.7 for F₂ and F₅, respectively as illustrated in Table 3, which is attributed to the slightly hydrophobic nature of leucine that might reduce the particle wetting hence retarding its

Table 3 Physicochemical Characteristics Of Reconstituted Spray-Dried Rifampicin Nanocomposites

Formula	Particle Size* (d-nm)	Particle Distribution Index*	Redispersibility Index*	Zeta Potential* (mV)
NS	473.5±15.8	0.598±0.03	4.7±0.16	-8.77±1.66
F ₁	111.2±2.97	0.483±0.04	1.1±0.03	-21.4±2.19
F ₂	123.9±3.95	0.552±0.05	1.2±0.04	-20.2±1.77
F ₃	208.1±2.72	0.532±0.06	2.0±0.04	-18.8±1.06
F ₄	221.0±3.46	0.319±0.01	2.2±0.03	-20.0±1.41
F ₅	277.7±3.21	0.440±0.07	2.7±0.03	-19.4±0.85
F ₆	147.5±4.16	0.462±0.05	1.5±0.04	-19.6±1.08
F ₇	177.6±2.72	0.479±0.03	1.7±0.04	-21.4±2.05

Note: *Mean±SD (n=3).

reconstitution. A further increase in leucine concentration (F_3) led to a higher RDI value of 2. This observation was in a close accordance with that reported by Wang et al,⁵⁰ where spray drying of levofloxacin lipid hybrid nanoparticles in the presence of leucine resulted in an increase of RDI value from 1.3 to 1.7.

Formula F_6 (1: 2 w/w maltodextrin/mannitol) showed an increase in the RDI value to 1.5 relative to that of F_2 (1.2), because of possible interactions and steric effects of maltodextrin. Otherwise, the addition of mannitol to the formulation (F_7) enhanced the powder re-dispersibility evidenced by a smaller RDI value of 1.7 in comparison to that of F_5 (2.7). Therefore, the protective action of matrix formers for the nanocomposites can be attributed to their function as a continuous solid matrix where nanocrystals were dispersed. Upon contact with water, the matrix former dissolved and nanocrystals were liberated in their free form.

Spray-Dried Powder Flowability

Flow property is considered as one of the promoting parameters in the successful aerosolization of the spray-dried powders. Good flowability of the powder is a prerequisite to generate adequate metering, dispersion, and fluidization of a dry powder from an inhaler device. Angle of repose (θ), Carr's index (CI), and Hausner ratio (HR) are considered indirect indicators to quantify powder flowability.²²

Rifampicin nanosuspension without any matrix former (NS) illustrated very poor flowability with values of 60.17°, 44.38% and 1.79 in terms of angle of repose, CI and HR, respectively. This poor flow behaviour of NS powder is due to its sticky nature and exhibition of strong interparticulate cohesion forces. In contrast, the usage of different carriers (F_1 – F_7) significantly improved the

powders flow properties as evidenced by the low θ , CI, and HR values (Table 4).

The use of mannitol (F_1) or maltodextrin (F_4) as a matrix former significantly decreased the values of flow indices as illustrated in Table 4 (p -value <0.05). F_1 showed passable to poor flowability according to θ and CI values, respectively. However, the powders obtained in the presence of maltodextrin (F_4) exhibited poor potential flow characteristics where the values of θ , CI, and HR were 48.1°, 33.12% and 1.49, respectively. This difference in flow properties may be attributed to the nature of the matrix formers used. It was proved that the high molecular weight maltodextrin has a cohesive nature, thus exhibiting poor flowability with high values of flow indices.⁵¹ Furthermore, the difference in flowability between (F_1) and (F_4) might be related to the surface morphology in general of the corrugated particles. It could be deduced that corrugated particles had lower interparticulate interactions than smooth particles, owing to reduced cohesion and contact between the particles, thus improving the flow properties. The obtained results were in a good agreement with previous studies.^{48,52–54}

L-leucine presence in the formulations (F_2 and F_5) was able to enhance powders flow properties. This effect is due to its potential ability to reduce powder cohesion through reduction of particle surface energy and water sorption. Additionally, leucine induced surface irregularities that could increase the inter-particle distance and increase the total surface area, thereby reducing the inter-particle interactions as reported in earlier findings.^{23,55} However, the flow improvement of formula F_3 with the highest leucine content was not significant due to higher morphological irregularity that negatively affects flowability. Sever particles surface irregularity tends to make the particles to stick together with a greater mechanical interlocking.

Table 4 Flow Features Of Spray-Dried Rifampicin Nanocomposites

Formula	Angle Of Repose* (θ)	Bulk Density* (g/cm^3)	Tapped Density* (g/cm^3)	Carr's Index* (%)	Hausner Ratio*
NS	60.17±4.05	0.089±0.005	0.160±0.008	44.38±5.39	1.79±0.16
F_1	41.80±1.09	0.129±0.003	0.178±0.007	27.53±2.09	1.38±0.04
F_2	32.63±2.03	0.145±0.004	0.177±0.003	18.08±1.03	1.22±0.02
F_3	36.24±2.18	0.149±0.008	0.194±0.003	23.19±3.87	1.30±0.07
F_4	48.10±3.15	0.103±0.006	0.154±0.007	33.12±3.18	1.49±0.13
F_5	37.58±1.19	0.172±0.004	0.227±0.009	24.23±4.04	1.32±0.07
F_6	34.06±1.63	0.161±0.008	0.199±0.004	19.09±3.14	1.23±0.05
F_7	31.83±2.93	0.151±0.008	0.183±0.005	17.49±3.87	1.21±0.04

Note: *Mean ± SD (n=3).

The combination of mannitol with maltodextrin in F₇ showed a good flow characteristic as evidenced by low θ , CI, and HR values of 31.83°, 17.49%, and 1.21, respectively. Unlikely, atorvastatin microemulsion co-sprayed with a mixture of dextran and mannitol showed a slight, non-significant decrease in the flowability indices compared to the use of either dextran or mannitol alone.²⁶

In-Vitro Dissolution Studies

Lung defense mechanisms can clear rifampicin inhaled powder due to its sparingly soluble nature at physiological pH. Therefore, enhancing RIF solubility in pulmonary lining fluid could induce supersaturation. This supersaturation of the pulmonary lining fluid, especially in microbial infiltration regions, can increase the fraction of RIF that is

penetrated the microbial cells and inhibit the microbial cytochrome p450. Moreover, it has previously been demonstrated that the increase in drug solubility has a direct positive impact on its antimicrobial in vivo activity.^{56–59} Dissolution profile of RIF raw powder and its spray-dried nanosuspension were compared to those of different SD-RIF nanocomposites formulations (F₁– F₇) and results are depicted in Figure 2.

Results revealed a significant enhancement of RIF release in PBS pH 7.4 from the studied formulations compared to raw RIF crystalline powder (*p*-value <0.05). Percentage of dissolved drug after 10 mins (Q_{10min}) was calculated for the studied samples. The slow dissolution rate of RIF (Q_{10min}=33.7% w/v) might be due to its highly hydrophobic nature that hindered its wettability by the

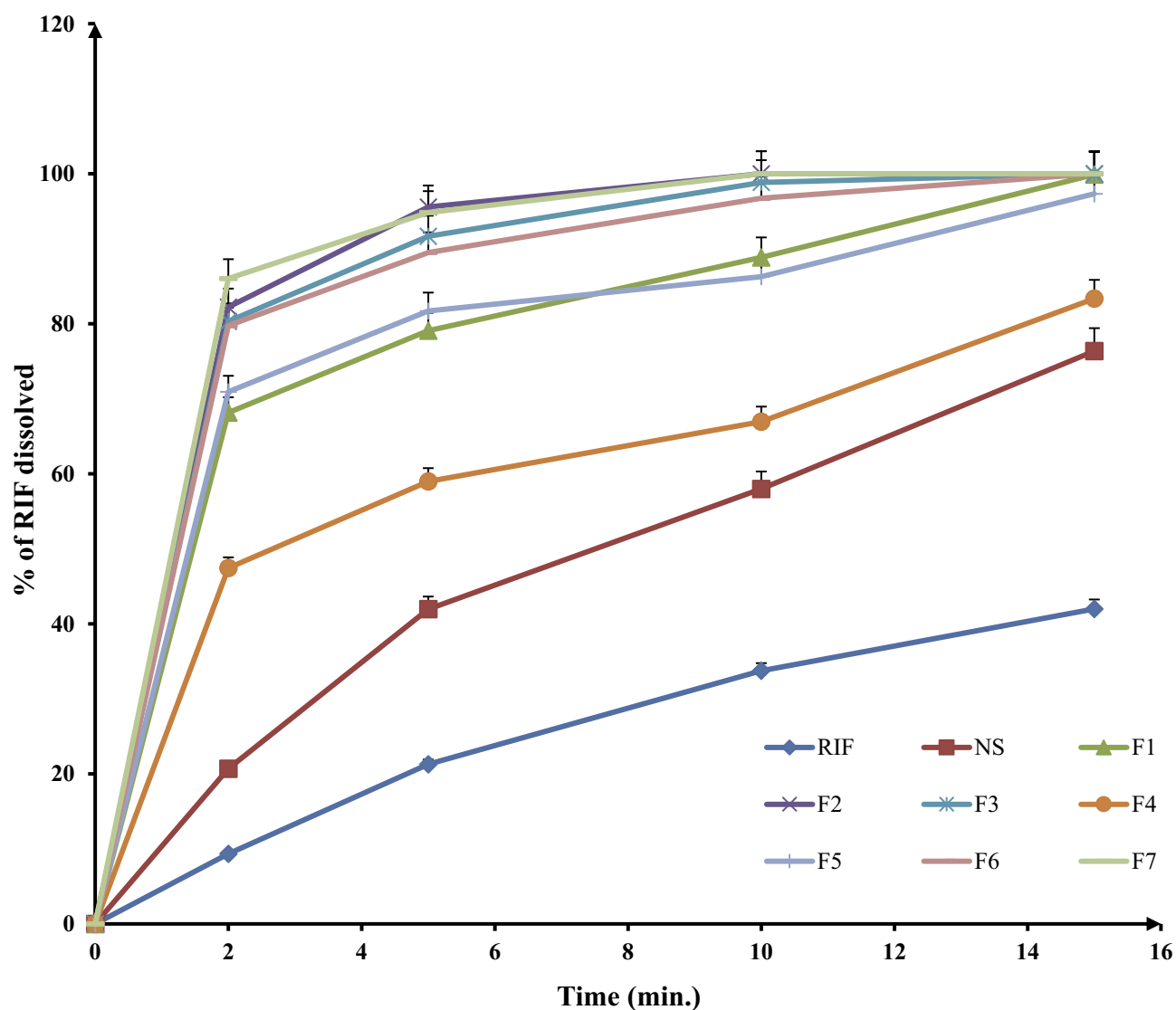


Figure 2 In-vitro dissolution profiles of different spray-dried rifampicin nanocomposites powders and crude rifampicin in PBS pH 7.4 at 37±2°C (mean±SD n=3).

aqueous dissolution media and encouraged particles agglomeration. On the other hand, the observed significant improvement of RIF dissolution from different nanocomposites formulations (Figure 2) could be correlated mainly to the particle size (Table 2). According to Noyes–Whitney equation, a progressive size reduction of the drug particles increases powder surface area resulting in an increased in its dissolution rate. Additionally, particle size reduction increases the dissolution velocity as a result of the reduction in the diffusion layer thickness surrounding the particles and the increase in the concentration gradient between the surface of the particle and the bulk which facilitate particle dissolution.⁶⁰ Other factors can contribute to RIF dissolution enhancement. Regarding the Ostwald–Freundlich equation, the increased particle-surface tension as a result of enhanced particle-surface curvature can consecutively increase particle solubility.²⁵ Furthermore, the process of RIF nanocomposite formation might lead to the formation of crystal defects. These crystal defects, including dislocations, influenced the crystal lattice energy and increased surface free energy thus enhanced RIF saturation solubility and dissolution.⁶¹ A similar finding was reported in the previous attempts.^{25,62,63} However, a decrease in the dissolution rate of spray-dried NS ($Q_{10\text{min}}=57.99\%$ w/v) was observed compared to the original aqueous nanosuspension ($Q_{10\text{min}}=97\%$ w/v), which highlighted the effect of drying process. It could be explained when observing spray-dried nanosuspension that remained floating on the surface of dissolution medium at the beginning of the dissolution test. This difference was diminished after approximately 30 mins as the dried NS was properly dispersed into the dissolution medium.

The nanocomposite matrix formers mannitol (F_1) or maltodextrin (F_4) significantly enhanced nanocrystals dispersibility, wettability as spray-dried powders did not float on the surface of dissolution medium and resulted in $Q_{10\text{min}}$ values of 88.84% and 66.95% w/v, respectively. These results were confirmed by reconstitution test that revealed a better wetting and higher re-dispersibility of formulas F_1 and F_4 compared to its matrix formers free formulation (NS). The enhanced wettability was able to improve the microenvironment surrounding RIF particle in which the saturation concentration was enhanced, accelerating its dissolution rate.

Mannitol-based spray-dried formulation (F_1) provided higher saturation levels of RIF compared to maltodextrin spray-dried NC (F_4) because of many probable facts. One of these facts was the variation in their particle size as

early illustrated in Table 2, where mannitol-based nanocomposites (F_1) showed a smaller particle size with larger surface area thus a faster dissolution rate. Furthermore, the hydrophilic nature of the mannitol allowed a good dispersion of RIF particles in the dissolution media, which could be a problematic for hydrophobic compounds as reported previously.^{13,25,64} In fact, during the spray-drying procedure, the carrier swelling might cause a deep and presumably viscous incorporation of the drug into the matrix network. It was proved that the viscosity of 10% w/v solution of maltodextrin is about 50 times higher than that of mannitol.⁶⁵ Consequently, the high viscosity of maltodextrin decreased the drug diffusion coefficient, resulting in a low dissolution rate from its spray-dried NCs (F_4) and induced a diffusion-controlled release mechanism. Presumably, the high viscosity of this carrier was the main factor controlling the drug dissolution rate. The same observation was reported by Valizadeh et al,⁶⁵ where the drying of indomethacin solid dispersion in the presence of dextrin delayed and decreased its dissolution behavior in comparison to that prepared with mannitol.

Leucine inclusion within the formulations (F_2 , F_3 , and F_5) significantly accelerated the RIF dissolution rate with $Q_{10\text{min}}$ values of 100%, 98.84%, and 86.27% w/v, respectively (p -value <0.05). This effect is totally different from that observed with similar formulations, in which a delayed dissolution profile with the inclusion of leucine was noticed.⁶⁶ Regardless of the slight hydrophobicity of leucine, the enhancement of dissolution profile could be mainly ascribed to the rising of particle corrugation as previously demonstrated in the SEM micrographs (Figure 1). The higher surface area accompanied with the corrugated particles might cause an increase in the solubility kinetic and consequently accelerated the dissolution rate of poorly soluble drugs. This observation was in a close accordance with a study revealed by Weiler et al.⁶⁷

The combination of maltodextrin to mannitol with a ratio of 1:2 w/w (F_6) delayed the dissolution rate of RIF but with a non-significant difference in comparison to that of F_2 (p -value >0.05). Otherwise, the addition of mannitol to the formulation (F_7) significantly improved the dissolution behavior of RIF with $Q_{10\text{min}}$ value of 100%w/v relative to the corresponding formulation (F_5 , $Q_{10\text{min}}=86.27\%$ w/v) (p -value=0.022) as a result of a better wettability accompanied by the use of mannitol.

The in-vitro dissolution parameters, namely dissolution efficiency at 10 mins (%DE_{10min}) and mean dissolution time (MDT) were used to compare the dissolution data of

all SD-RIF nanocomposites as depicted in Figure 3. DE and MDT values can be of benefit in translating a whole dissolution curve into a single number and hence comparison can be carried out easily between large numbers of formulations. %DE was calculated from the area under the dissolution curve up to time point and expressed as a percentage of the area of the rectangle described by 100% at the same time point.

The dissolution efficiency at 10 mins (%DE_{10min}) is the lowest for raw RIF crystalline powder (19.28%) and increased remarkably for the SD-nanocomposites without matrix formers (NS, 36.2%). Further increase was obtained with formulations containing matrix formers either mannitol (F₁, 70.89%) or maltodextrin (F₄, 52.19%) and even more for the SD-nanocomposites containing leucine (F₂, F₃, and F₅) with %DE value of 84.78%, 81.45%, and 71.98%, respectively (Figure 3). Formula F₇ containing a mixture of mannitol, leucine, and maltodextrin showed a high %DE value of 83.78% but with non-significant difference to both F₂ and F₃ (*p*-value >0.05). The results of MDT were in accordance with %DE_{10min} where the RIF powder revealed the highest mean dissolution time

(53 mins) while SD-nanocomposites (F₂ and F₇) exhibited the lowest MDT values of 1.56 and 1.62 mins, respectively.

Dissolution testing highlighted that SD-nanocomposites were able to provide faster RIF dissolution rates compared to the raw crystalline powder in turn achieving a higher drug fraction available for absorption. This is a special merit for RIF because its in-vivo dissolution is the rate-limiting step in its absorption as it is a class II drug according to the biopharmaceutics classification system (BCS). Thus, the improved in-vitro dissolution of SD-nanocomposites may result in enhanced in-vivo bioavailability of RIF. This is consequential in oral and pulmonary delivery of SD-nanocomposites of poorly water-soluble drugs.

Aerosolization Performance Of SD-RIF NCs

Inhalation-based therapeutic approach applied to treat pulmonary TB chief advantage is its ability to deliver entire accurate dose of the antimicrobial agent directly to the site of infection with minimal systemic exposure. But the obstacle facing this approach is controlling the administered powder deposit site. RIF particles generated from the

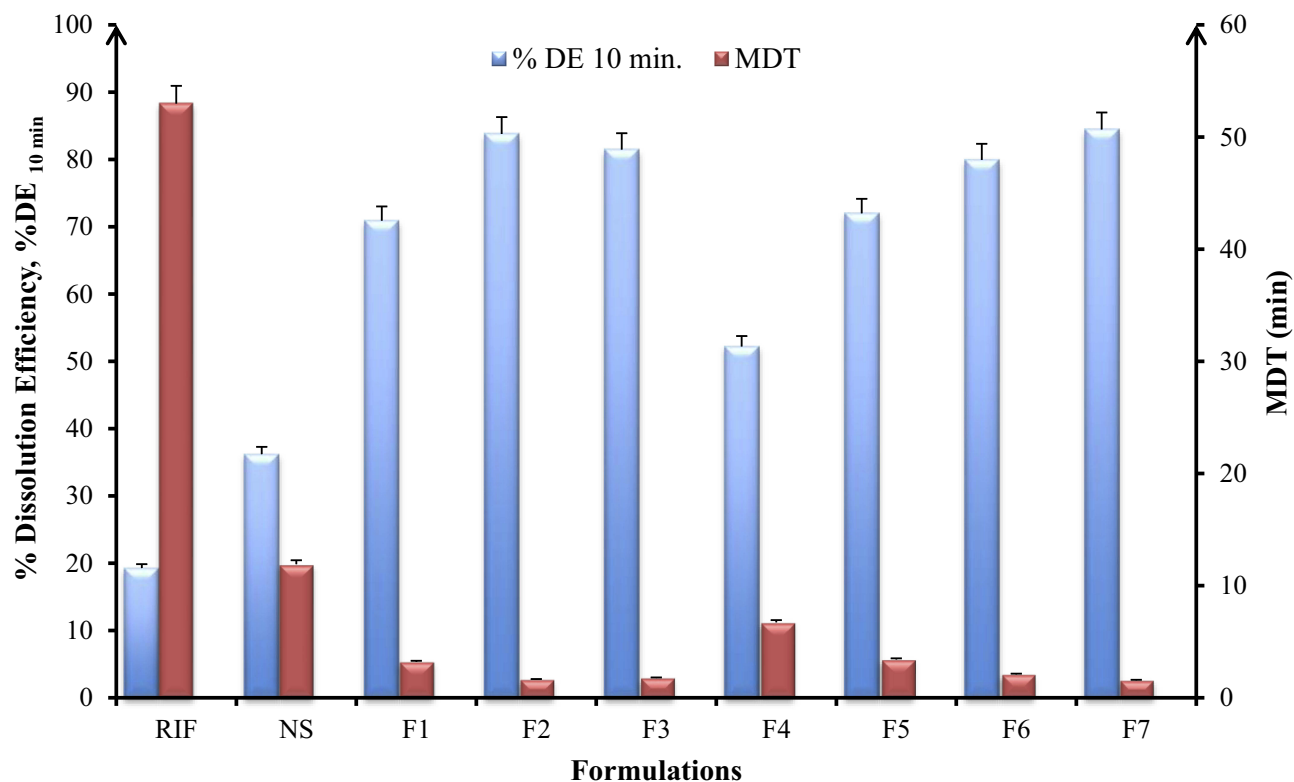


Figure 3 In-vitro dissolution parameters; dissolution efficiency, %DE at 10 min and mean dissolution time, MDT of spray-dried rifampicin nanocomposites prepared with different matrix formers and raw rifampicin powder (mean±SD n=3).

inhaler device should penetrate the lung deeply to reach the infection site. Therefore, the DPI formulation strategy requires the preparation of aerosols that can be readily emitted off the inhaler, while at the same time possesses aerodynamic diameters (d_{ae}) between 1 and 5 μm for effective deposition in the lower respiratory tract.⁶⁸

To evaluate the effect of particle characteristics and formulation variables on SD-nanocomposites aerosolization properties, in-vitro deposition of RIF containing formulae had been evaluated using a TSI at a flow rate of 60 L/min. The inhalation parameters exhibited noticeable differences due to the incorporation of matrix formers and dispersibility enhancers as shown in Table 5. The improved aerosolization properties were indicated by higher values of %EF, %RF, %EI, and a lower calculated d_{ae} .¹³ SD-nanosuspension without matrix former (NS) revealed significantly higher aerodynamic diameter (9.17 μm) (p -value <0.05), probably due to the stickiness and hygroscopic behavior of the powder. However, the SD-nanocomposites (F₁-F₇) showed smaller aerodynamic diameters ranging from 1.46 (F₂) to 2.99 (F₃), predicating effective aerosolization properties. Furthermore, in comparison to NS, the inclusion of matrix formers (F₁-F₇) raised the emitted fraction (%EF) delivered from the inhaler from 60.7 (NS) to 95.22% (F₇) and consequently, elevated the amount of drug deposited in the lower respiratory tract (%RF) from 19.03 (NS) to 65.41% (F₇) and effective inhalation index (%EI) from 25.72 (NS) to 77.93% (F₇).

However, the SD-nanocomposites (F₁-F₇) possessed aerodynamic diameters in the respirable range, their inhalation parameters were varied (Table 5). The %EF ranged from 78.42 (F₄) to 95.22% (F₇) and the %RF varied from 40.12 (F₄) to 65.41 (F₇). These differences might be related to their variation in the flow properties as early illustrated (Table 4). With regard to Figure 4, there was an inverse

relation between either the dose emitted from the inhaler (%EF) or the respirable fraction (%RF) and the angle of repose of SD-nanocomposites powders with a correlation coefficient value (R^2) of 0.9524 and 0.9851, respectively. It was found that a good flow powder evidenced by a low angle of repose value exhibited a high-emitted fraction and thus, enhanced the particles deposition in the lower respiratory tract.

The in-vitro distribution after delivery of SD-nanocomposites with an Aerolizer attached is illustrated in Figure 5. The SD-nanosuspension without matrix formers (NS) exhibited a high device and mouth/throat deposition (39.3% and 34.5%, respectively) with a low amount deposited in stage 2 (10.9%), confirming the low ability of these particles to be aerosolized. After inhalation by a patient, a portion of these nanocrystals would be stopped in the oropharyngeal region and removed by the mucociliary clearance from the trachea or by swallowing into throat. This observation was probably due to the formation of stable large agglomerates as a result of high powder hygroscopicity, which promoted aggregation of the individual particles. These stable large un-aerosolized agglomerates evidenced by the SEM micrographs and laser diffraction measurements.

However, the inclusion of mannitol or maltodextrin as matrix former enhanced the deposition pattern of SD-nanocomposites due to their ability to reduce the hygroscopicity of the powders through the formation of a protective layer on the particle surface that would prevent particles adhesion and the subsequent large agglomerates assembly. This finding was in accordance with earlier study reported by Malamatarı et al.¹³ The use of mannitol as a matrix former (F₁) showed a lower deposition in the mouth and throat regions and thus, upon inhalation, could deposit deeply in the lungs evidenced by a high RF value (49.91%) relative to

Table 5 Aerosol Dispersion Performance Parameters Of Spray-Dried Rifampicin Nanocomposites

Formula	Aerosol Dispersion Performance Parameters			
	Calculated d_{ae} * μm	EF* % w/w	RF* % w/w	EI* % w/w
NS	9.17±1.45	60.70±3.04	19.03± 4.33	25.72±3.29
F ₁	2.16±0.09	81.14±2.43	49.91± 2.49	57.39±3.44
F ₂	1.46±0.18	90.46±1.05	59.90±4.98	70.04±4.20
F ₃	2.99±0.29	85.20±4.26	53.01±3.71	60.53±3.03
F ₄	2.45±0.08	78.42±2.35	40.12±3.61	49.70±3.97
F ₅	2.07±0.21	82.69±1.65	57.19±4.57	62.54±2.50
F ₆	2.13±0.44	89.01±3.56	58.52±2.34	68.10±4.41
F ₇	1.65±0.32	95.22±1.90	65.41±2.62	77.93±3.17

Notes: * D_{ae} , aerodynamic diameter. Mean±SD (n =3).

Abbreviations: EF, emitted fraction; RF, respirable fraction; EI, effective inhalation index.

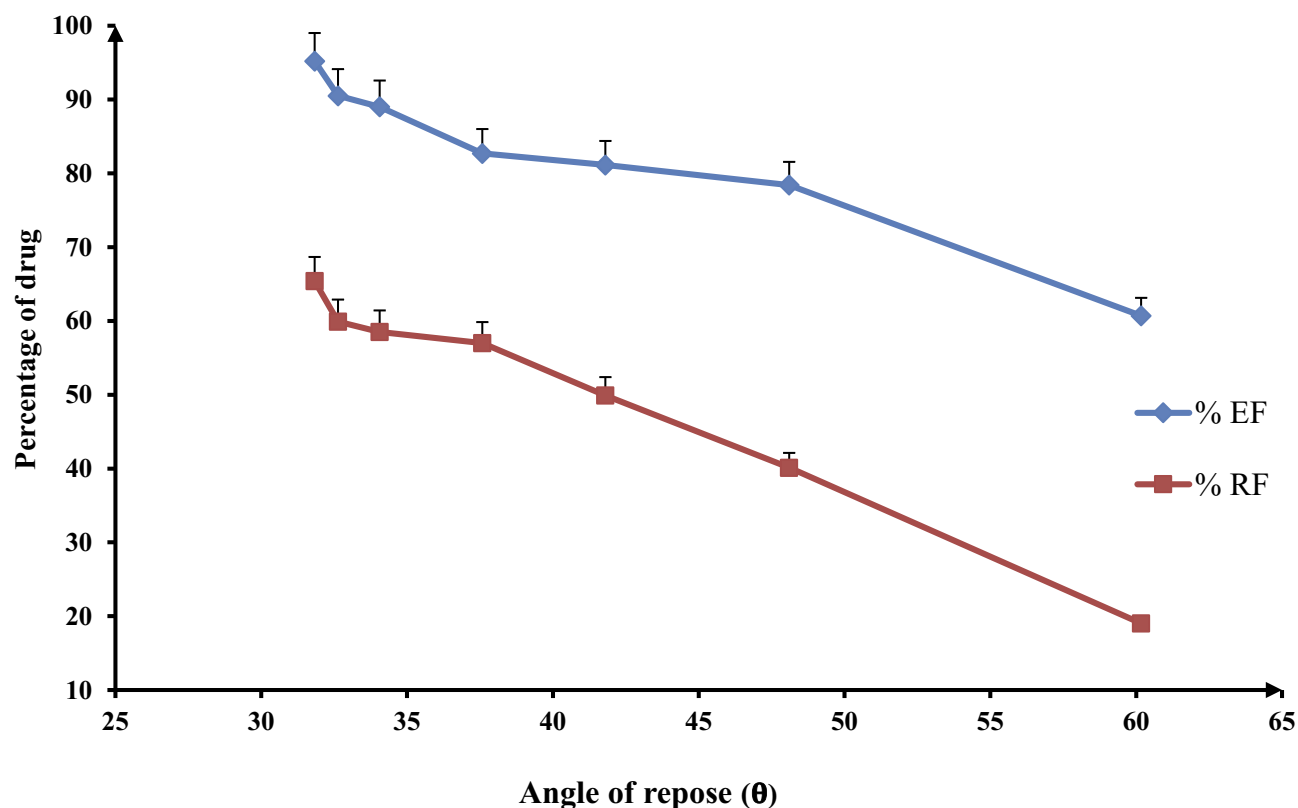


Figure 4 Effect of the flow properties on the inhalation indices of spray-dried rifampicin nanocomposites, namely emitted fraction (%EF) and respirable fraction (%RF), mean \pm SD (n=3).

the corresponding formulation of maltodextrin (F_4). The variation in their aerosolization performance could be explained according to the particles characteristics that conducted from the early-illustrated results. Mannitol yielded particles (F_1) with better flow properties, lower geometric and aerodynamic diameter in comparison to the maltodextrin formulation. Furthermore, the corrugations and asperities present on the surface of F_1 particles could decrease the true surface area of the contact between the particles reducing the cohesion between the individual particles. Similarly, a study reported by Chew et al,⁵⁴ who concluded that corrugated particles could enhance aerosol performance over the smooth spherical particles of otherwise similar physical properties. Thus, surface roughness or irregularity of mannitol modified spray-dried powders (F_1) could justify their enhanced aerosolization properties.

Moreover, leucine incorporation into the formulations (F_3 and F_5) led to better aerosolization properties indicated by the higher RF values of 59.9% and 57.19%, respectively, relative to the leucine free formulations (F_1 and F_4 , respectively). As a result of leucine hydrophobic nature, its presence was anticipated to limit SD-nanocomposites moisture uptake,

which would render the particles less cohesive and hence improving the aerosolization efficiency.⁶⁶ Moreover, leucine has a surface activity which enhanced particles dispersibility through shell formation around the particles surface during drying.¹³ Furthermore, through its surface activity, leucine had been found to lower the surface free energy therefore reducing the particles tendency to agglomerate.⁶⁶ The same observation was noticed by Osman et al,⁴⁰ where the spray drying of DNase microparticles in the presence of leucine raised the emitted fraction from 75% to more than 96% with a high stage 2 deposition corresponding to RF of 68%. More specifically, the addition of leucine on a mannitol or maltodextrin-based spray-dried powder (F_2 or F_5 , respectively) for inhalation was found to enhance the performance of dry powder inhaler formulations, by forming a coating on the dry particle surface preserving the individual particles as collected from the dryer, preventing any particle fusion. Therefore, the property of leucine on improving dispersibility of particles and thus reducing their cohesiveness might explain the remarkably reduced throat and mouth deposition. In addition, leucine inclusion was known to produce particles with corrugated surfaces upon drying, which reduce inter-particulate contact

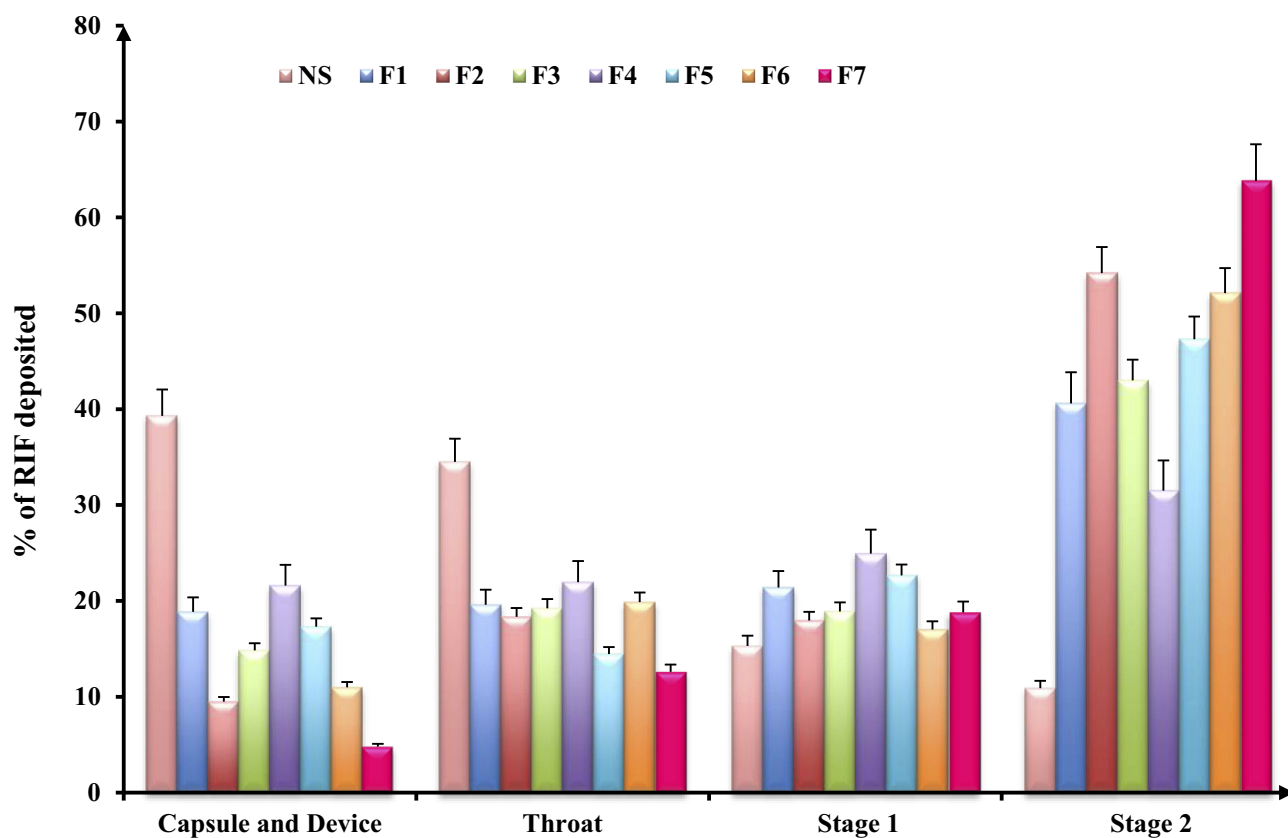


Figure 5 In-vitro deposition data of rifampicin-loaded spray-dried nanocomposites powders determined using a twin stage impinger. Aerolizer® (DPI) was used to deliver the dose into the various parts of the TSI operated at a flow rate of 60 L/min, mean±SD (n=3).

surface areas, resulting in better particle dispersions as previously demonstrated in the SEM micrographs (Figure 1).

The incorporation of mannitol to maltodextrin in the formulation (F₇) revealed the best aerosolization performance with very little device and throat deposition (4.8% and 12.6% w/w, respectively) together with high RF value of 65.41% w/w as a result of good flow property and small geometric and aerodynamic diameter accompanied by this formula. Otherwise, F₆ exhibited non-noticeable difference in the in-vitro lung deposition data relative to the corresponding formulation (F₂) as shown in Figure 5. Therefore, and according to the obtained results, formula F₇ was chosen as optimum DPI formulation for effective RIF lower respiratory tract deposition.

Drug-Excipient Compatibility Studies

Differential Scanning Calorimetry (DSC)

DSC analysis employed to investigate any physical change in the crystalline state and thermal behavior of RIF upon drying process. The DSC thermograms of raw RIF powder, maltodextrin, mannitol, leucine, spray-dried RIF NCs (F₇), and the physical mixture are depicted in Figure 6.

Maltodextrin thermograms revealed no endothermic peaks indicating its amorphous structure. Otherwise, leucine and mannitol thermograms exhibited a single endothermic peak with single melting point at 254°C and 164.64°C. RIF showed a single exothermic peak at 263°C as previously reported.²⁰ This characteristic peak of RIF was observed in the physical mixture thermogram as well as the endothermic peaks of the other components. Moreover, in case of SD-RIF NCs, the characteristic exothermic peak was obviously broadened reflecting certain decrease in drug crystallinity. DSC results proposed a reduction in RIF crystallinity upon spray-drying process.

Fourier Transform Infrared (FTIR) Spectroscopy

For further detection of any possible change and chemical interaction with RIF and the SD-RIF NCs solid-state, IR spectra of RIF, mannitol, maltodextrin, leucine, SD-RIF NCs (F₇), and the physical mixture in the same ratio of amounts found in F₇ are illustrated in Figure 7. RIF spectrum showed absorption bands at 3482, 2878, 1726, 1643, and 1566 cm⁻¹ attributable to hydroxyl, N-methyl, acetyl carbonyl, furanone carbonyl, and amide carbonyl groups,

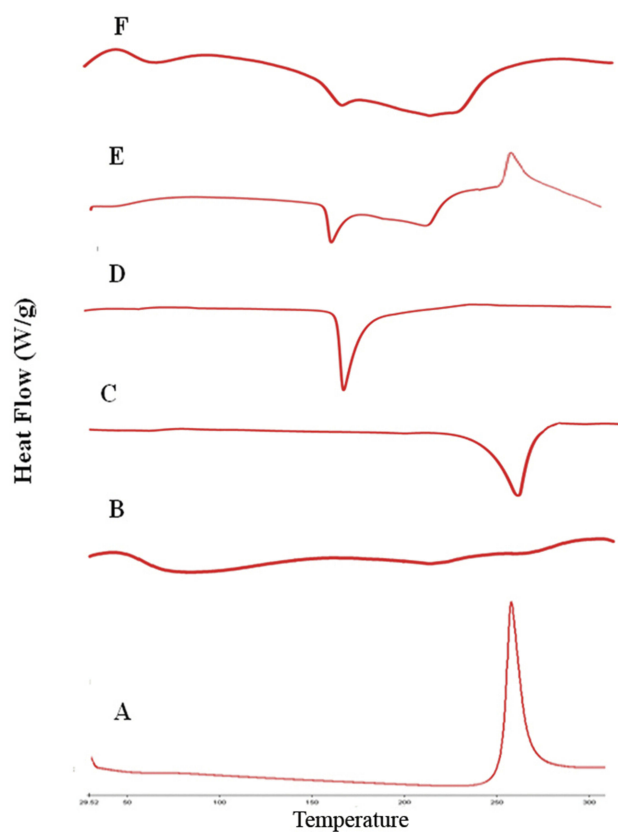


Figure 6 DSC thermograms of rifampicin-loaded spray-dried nanocomposites powder with its individual components, rifampicin (A), maltodextrin (B), leucine (C), mannitol (D), physical mixture (E) and formula F₇ (F).

respectively as reported by Agrawal et al.⁶⁹ The IR spectrum of pure maltodextrin revealed the band at 3397 cm^{-1} due to O–H stretching, at 2928 cm^{-1} attributed to the sp^3 C–H stretching, at 1647 cm^{-1} assigned to C–O stretching and 1419 cm^{-1} due to CH_2 bending. Further, pure maltodextrin spectrum presented peaks of 1153 , 1080 , and 931 cm^{-1} . The peaks of 1153 and 1080 cm^{-1} are caused by stretching of the C–O bond and the 931 cm^{-1} peak due to the angular deformation of the CH and CH_2 bonds, all from groups found in the carbohydrates.^{70,71} Mannitol showed a broad band at $3392\text{--}3291\text{ cm}^{-1}$ relating to O–H stretching vibration as well as a band at 2967 due to C–H stretching. The OH plane deformation of 1st and 2nd alcohol was attributed to peaks 1280 and 1261 cm^{-1} . The peaks at 1082 and 1019 are caused by 1st and 2nd alcohol CO stretching. Furthermore, bands at 952 , 929 , 878 , 629 , and 414 represented the fingerprint of mannitol.⁷² The aerosolization enhancer L-leucine molecules exhibited at 2958 cm^{-1} due to its methyl group characterized by aliphatic CH_3 , at 1514 cm^{-1} assigned to the bending vibration of N–H band and at 1583 cm^{-1} attributed to the stretching mode of carbonyl group which is confirmed by the

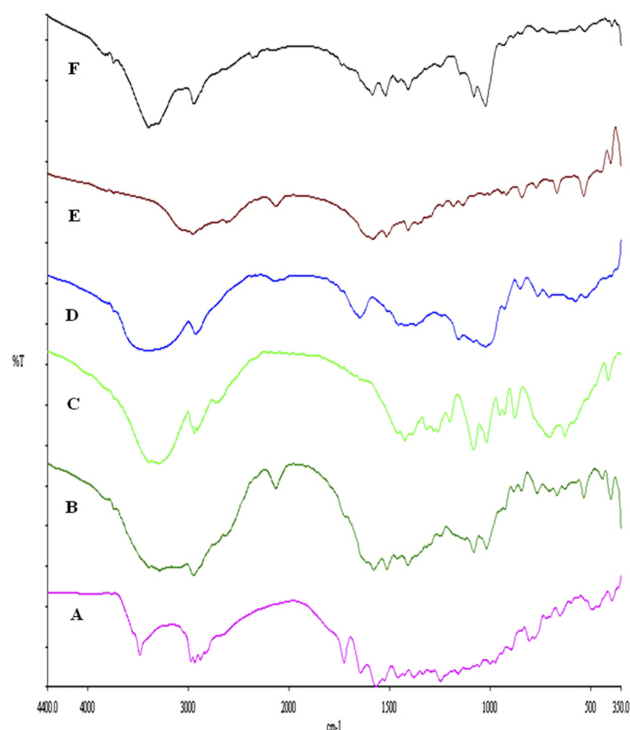


Figure 7 FTIR spectra of rifampicin-loaded spray-dried nanocomposites powder (F₇) with its individual components, rifampicin (A), physical mixture (B), mannitol (C), maltodextrin (D), leucine (E) and formula F₇ (F).

appearance of medium intensity band at 1408 cm^{-1} assigned to COO–asymmetric vibration as previously reported by Ishak and Osman.²⁶ The FT-IR spectrum of SD-RIF NCs (F₇) and the physical mixture of its components depicted in Figure 7 F and B showed the disappearance of characteristic RIF peaks. This could be due to overlapping of the drug by the presence of excess carriers. The same observation was reported by Ishak and Osman,²⁶ where the characteristic peaks of atorvastatin disappeared in the IR spectrum of spray-dried self-microemulsifying powders.

X-Ray Diffraction Of Powders

The X-ray diffractograms of the RIF, leucine, mannitol, maltodextrin, their physical mixture, spray-dried nanosuspensions (NS), and spray-dried RIF nanocomposites (F₇) are shown in Figure 8. Diffraction pattern of RIF exhibited intense peaks at 2θ of 13.65° and 14.35° , reflecting the crystalline nature of raw RIF. These characteristic peaks were corresponding to that of form I as early proved in DSC results. Maltodextrin illustrated a hollow pattern, revealing its amorphous state, while for mannitol, X-ray pattern was characteristic for its β -form (2θ : 10.5° , 14.9° , 17.1° , 21.5° , 23.7° , 29.7°).¹³ In addition, L-leucine diffractogram exhibited intense peaks at 2θ of

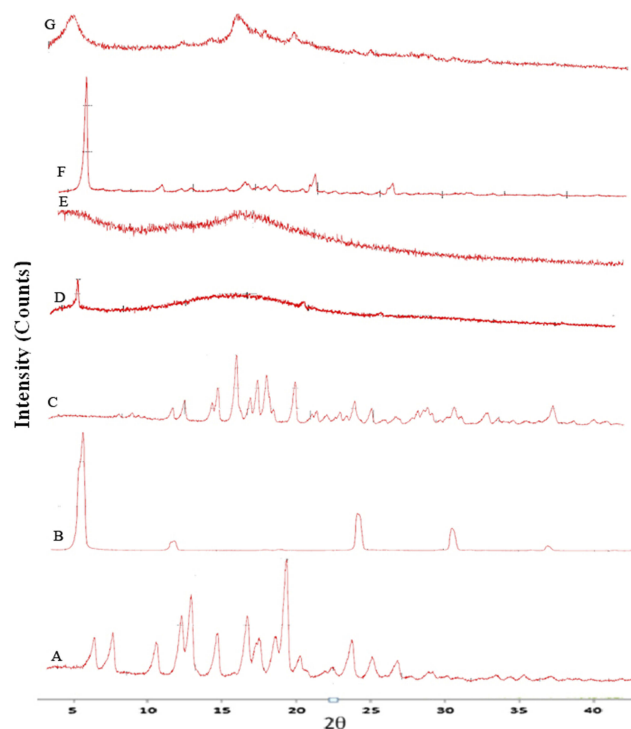


Figure 8 X-ray powder diffraction patterns of rifampicin (A), leucine (B), mannitol (C), maltodextrin (D), spray-dried rifampicin nanosuspensions (NS) (E), physical mixture (F) and spray-dried RIF nanocomposites (F₇) (G).

6.07°, 24.3°, and 30.6° as early reported.⁷³ Their physical mixture pattern showed the characteristic RIF peaks. However, the X-ray profiles of SD-nanosuspension (NS) and SD-RIF NCs (F₇) exhibited a significant reduction in the intensities as well as broadening of the characteristic peaks. Thus, results obtained from DSC and X-ray analysis proposed the potential of spray drying process to convert RIF from its crystalline unprocessed form into a partially amorphous nanometric form.

In-Vitro Cytotoxicity Study

With the evolving of modern drug delivery systems, cytotoxicity assessment of such formulations becomes an indispensable aspect to be addressed. While an accurate toxicity determination of a formulation can only be determined in-vivo, a variety of in-vitro toxicological assays, performed on adequately selected cell lines, might provide useful information and are widely accepted as primary indicators. The evaluation of the biocompatibility of nanocomposites and corresponding raw materials was performed by means of the metabolic activity (MTT) assay. Nanocomposites as drug delivery systems have attracted unique functional characteristics defined by their size-related properties. These outstanding features such as

hydrophobicity, surface charge, optical and magnetic properties or catalytic activity can affect their safety on the tissues. Therefore, their toxicity against A549 human alveolar epithelial cells has been investigated using in-vitro MTT cytotoxicity assay. This assay had been known to indicate the level of mitochondrial dehydrogenase enzymes that is still metabolically active. The cell viability exhibited a concentration-dependent activity that decreased with raising RIF concentration. However, it was obvious that the percentage of cell cytotoxicity in the presence of RIF NS and SD-RIF NCs was clearly lower than that obtained with free RIF at all the concentrations tested (Figure 9) which suggested the safety of the used excipients. RIF-NCs had relatively low cytotoxicity with concentrations less than 1 mg/mL, whereas the concentration of RIF reported to be used for the tuberculosis therapy was 5 µg/mL.⁷⁴

The half-maximal inhibitory concentration (IC₅₀) was obtained from the concentration-dependent cell viability curves. IC₅₀ values were 0.5±0.027, 0.8±0.015, 0.73±0.03, 0.72±0.03, 0.74±0.04, and 0.67±0.04 mg/mL for free RIF, RIF NS, F₂, F₅, F₆, and F₇, respectively. The IC₅₀ values of RIF NS and different SD-nanocomposites showed a non-significant difference (*p*-value >0.05) and were significantly higher than that of free RIF (*p*-value <0.05). These results could be attributed to a slower cellular uptake of the nanocomposites in comparison to free RIF. The cellular uptake of nanocrystals may occur by either receptor-mediated or non-specific endocytosis.⁷⁵ The former, likely the clathrin- and caveolae-mediated endocytosis, required a specific transport ligand while the latter depended on the morphological and physicochemical characteristics of the nanocomposites.^{75,76} The surface charge of the nanocomposites implied an important role in the cellular uptake. Mahmoud et al⁷⁷ proved that the cellular uptake of positively charged cellulose nanocomposites via human embryonic kidney 293 was superior to those of the negatively charged one. The authors attributed that to the repulsive force between the negatively charged cell membrane and the nanocomposites. In accordance, the slower uptake of RIF NCs and NS is probably due to either the absence of active transport ligand or the presence of a negative charge on its surface. Thus, RIF bearing NS showed a promising candidate for lowering the drug toxicity against A549 cells.

Storage Stability Study Of SD-RIF NCs

To check the storage stability of SD-RIF NCs (F₇), the powder was kept in a desiccator at room temperature for 6 months. Physicochemical characteristics of SD-RIF NCs including

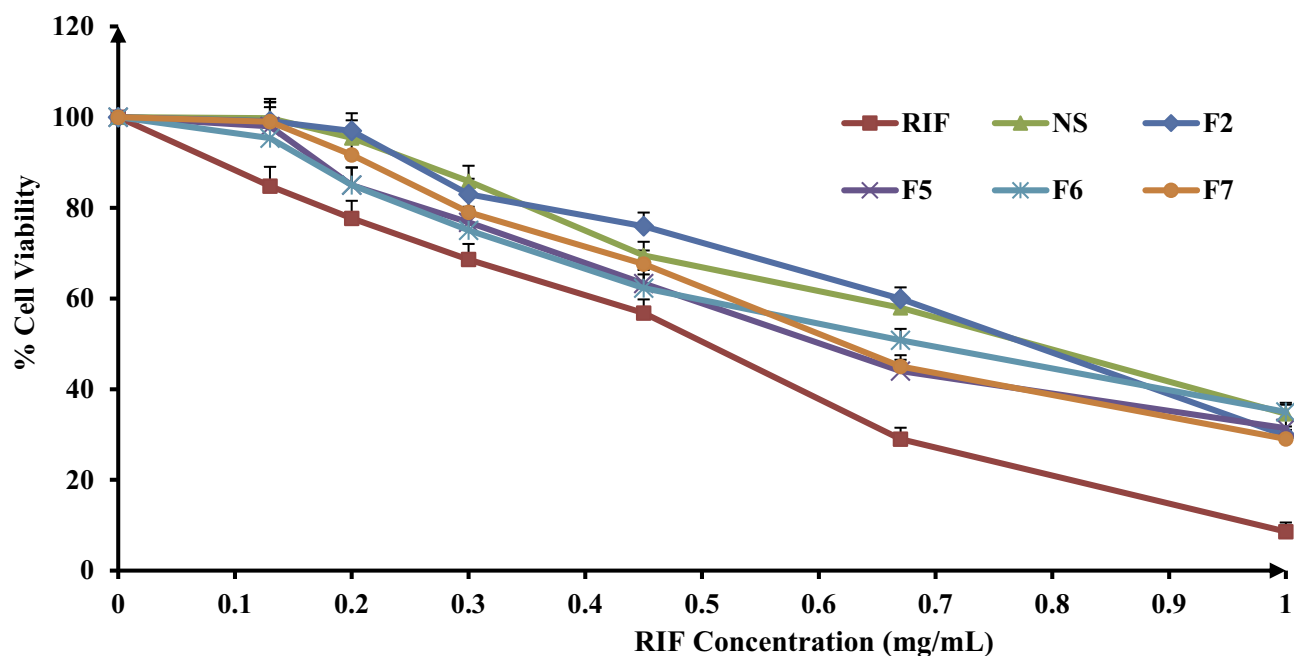


Figure 9 Percentage of viability of A549 cells measured by the MTT cytotoxicity assay after exposure for 24 hrs to various concentrations of free rifampicin, rifampicin nanosuspensions and spray-dried rifampicin nanocomposites (F₂, F₅, F₆, F₇) at 37±0.5°C, mean±SD (n=3).

drug content (%DC), particle size, Pdl, Zeta potential, tapped density and $Dv_{50\%}$ were evaluated. Furthermore, the theoretical aerodynamic diameter was calculated using the tapped density and $Dv_{50\%}$ of SD powders in order to predict their aerosolization performance (Table 6). There were non-significant changes in the physicochemical characteristics of SD-RIF NCs (F₇) stored within a period of 6 months reflecting high storage stability of the prepared formulation. For a further stability study, the effect of storage on the in-vitro dissolution profile of SD-RIF NCs (F₇) was evaluated. The in-vitro dissolution of SD-RIF nanocomposites showed unnoticeable alteration when stored for 6 months at room temperature. Almost superimposed dissolution patterns before and after storage furnished further evidence for the integrity of SD-nanocomposites within a period of 6 months.

Conclusion

Formulation of anti-tuberculosis drug rifampicin as a dry powder inhaler in combination with selected excipients for its pulmonary delivery could enhance its efficacy. Spray

drying technique was utilized to fabricate rifampicin-loaded nanocomposites utilizing its aqueous nanosuspension as a starting material hypothesizing that the nanocomposite powders are capable of dispersing and extricate original NS within the lung microenvironment. Combinations of matrix formers viz. mannitol and maltodextrin with or without leucine were evaluated. A novel dry powder composite assembly made up with maltodextrin, mannitol, and leucine at ratio of 2:1:1 was able to achieve a high powder yield, acceptable flowability and lower particle size and size distribution of both the spray-dried powders and the recovered nanosuspension. Furthermore, the spray-dried rifampicin nanocomposite exhibited a rapid dissolution rate with a high % DE_{10min} value of 83.78% and MDT value of 1.62 mins. The development of spray-dried rifampicin nanocomposite revealed a desirable microstructure for efficient deep lung deposition with good aerosolization characteristics evidenced by high values of %EF (95.22%), %RF (65.41%), and %EI (77.93%). Moreover, the incorporation of rifampicin in the nanocomposite particles allowed regulation of the drug/cell

Table 6 Stability Study Of Spray-Dried Rifampicin Nanocomposites (F₇) Stored At Room Temperature (25±2°C) For 6 Months

Time (Month)	DC (%)	z-Average (d-nm)	Pdl	ZP (mV)	ρ_{tap} (g/cm ³)	$Dv_{(50\%)}$ (μm)	d_{ae} (μm)
0	99.2±3.32	177.6±2.723	0.479±0.030	-21.4±2.05	0.183±0.005	3.85±0.77	1.65±0.32
6	97.4±0.54	177.9±4.711	0.474±0.027	-20.1±0.42	0.185±0.009	3.81±0.73	1.64±0.30

Note: Data are presented as mean±SD (n=3).

Abbreviations: DC, drug content; Pdl, particle distribution index; ZP, Zeta potential; ρ_{tap} , tapped density; d_{ae} , aerodynamic diameter.

interaction reducing the drug toxicity against A549 cells. Presumably, the novel developed dry powder nanocomposite system represents an auspicious beginning for anti-tuberculosis drugs optimal lung delivery.

Disclosure

The authors report no conflicts of interest in this work.

References

- Elsayed I, AbouGhaly MH. Inhalable nanocomposite microparticles: preparation, characterization and factors affecting formulation. *Expert Opin Drug Deliv*. 2016;13(2):207–222. doi:10.1517/17425247.2016.1102224
- Muralidharan P, Malapit M, Mallory E, Hayes D Jr., Mansour HM. Inhalable nanoparticulate powders for respiratory delivery. *Nanomedicine*. 2015;11(5):1189–1199. doi:10.1016/j.nano.2015.01.007
- Manca ML, Valenti D, Sales OD, Nacher A, Fadda AM, Manconi M. Fabrication of polyelectrolyte multilayered vesicles as inhalable dry powder for lung administration of rifampicin. *Int J Pharm*. 2014;472(1–2):102–109. doi:10.1016/j.ijpharm.2014.06.009
- Sosnik A, Carcaboso ÁM, Glisoni RJ, Moreton MA, Chiappetta DA. New old challenges in tuberculosis: potentially effective nanotechnologies in drug delivery. *Adv Drug Deliv Rev*. 2010;62(4–5):547–559. doi:10.1016/j.addr.2009.11.023
- Sagalowicz L. *Global Tuberculosis Control: Surveillance, Planning, Financing*. WHO; 2012.
- Padayatchi N, Friedland G. Decentralised management of drug-resistant tuberculosis (MDR- and XDR-TB) in South Africa: an alternative model of care. *Int J Tuberc Lung Dis*. 2008;12(8):978–980.
- Muttill P, Wang C, Hickey AJ. Inhaled drug delivery for tuberculosis therapy. *Pharm Res*. 2009;26(11):2401–2416. doi:10.1007/s11095-009-9957-4
- Shegokar R, Al Shaal L, Mitri K. Present status of nanoparticle research for treatment of tuberculosis. *J Pharm Pharm Sci*. 2011;14(1):100–116.
- Caminero JA, Sotgiu G, Zumla A, Migliori GB. Best drug treatment for multidrug-resistant and extensively drug-resistant tuberculosis. *Lancet Infect Dis*. 2010;10(9):621–629. doi:10.1016/S1473-3099(10)70139-0
- Mehanna MM, Mohyeldin SM, Elgindy NA. Respirable nanocarriers as a promising strategy for antitubercular drug delivery. *J Control Release*. 2014;187:183–197. doi:10.1016/j.jconrel.2014.05.038
- Sung JC, Pulliam BL, Edwards DA. Nanoparticles for drug delivery to the lungs. *Trends Biotechnol*. 2007;25(12):563–570. doi:10.1016/j.tibtech.2007.09.005
- Pandey R, Khuller GK. Antitubercular inhaled therapy: opportunities, progress and challenges. *J Antimicrob Chemother*. 2005;55(4):430–435. doi:10.1093/jac/dki027
- Malamatari M, Somavarapu S, Bloxham M, Buckton G. Nanoparticle agglomerates of indomethacin: the role of poloxamers and matrix former on their dissolution and aerosolisation efficiency. *Int J Pharm*. 2015;495(1):516–526. doi:10.1016/j.ijpharm.2015.09.013
- Watts AB, Williams RO III. *Nanoparticles for Pulmonary Delivery. Controlled Pulmonary Drug Delivery*. Springer; 2011:335–366.
- Yang Y, Cheow WS, Hadinoto K. Dry powder inhaler formulation of lipid-polymer hybrid nanoparticles via electrostatically-driven nanoparticle assembly onto microscale carrier particles. *Int J Pharm*. 2012;434(1–2):49–58. doi:10.1016/j.ijpharm.2012.05.036
- Tomoda K, Ohkoshi T, Kawai Y, Nishiwaki M, Nakajima T, Makino K. Preparation and properties of inhalable nanocomposite particles: effects of the temperature at a spray-dryer inlet upon the properties of particles. *Colloids Surf B Biointerfaces*. 2008;61(2):138–144. doi:10.1016/j.colsurfb.2007.07.016
- Tomoda K, Ohkoshi T, Hirota K, et al. Preparation and properties of inhalable nanocomposite particles for treatment of lung cancer. *Colloids Surf B Biointerfaces*. 2009;71(2):177–182. doi:10.1016/j.colsurfb.2009.02.001
- Tomoda K, Ohkoshi T, Nakajima T, Makino K. Preparation and properties of inhalable nanocomposite particles: effects of the size, weight ratio of the primary nanoparticles in nanocomposite particles and temperature at a spray-dryer inlet upon properties of nanocomposite particles. *Colloids Surf B Biointerfaces*. 2008;64(1):70–76. doi:10.1016/j.colsurfb.2008.01.016
- Yang M, Yamamoto H, Kurashima H, et al. Design and evaluation of poly(DL-lactic-co-glycolic acid) nanocomposite particles containing salmon calcitonin for inhalation. *Eur J Pharm Sci*. 2012;46(5):374–380. doi:10.1016/j.ejps.2012.02.024
- Mohyeldin SM, Mehanna MM, Elgindy NA. The relevancy of controlled nanocrystallization on rifampicin characteristics and cytotoxicity. *Int J Nanomed*. 2016;11:2209–2222.
- Singh C, Koduri LVSK, Singh A, Suresh S. Novel potential for optimization of antitubercular therapy: pulmonary delivery of rifampicin lipospheres. *Asian J Pharm Sci*. 2015;10(6):549–562. doi:10.1016/j.ajps.2015.08.003
- The United States Pharmacopoeia. Thirty Eight Ed: *The National Formulary, the Official Compendia of Standards*. Washington, DC: United States Pharmacopoeial Convention, Inc.; 2015:1327–1329.
- El-Gendy N, Berkland C. Combination chemotherapeutic dry powder aerosols via controlled nanoparticle agglomeration. *Pharm Res*. 2009;26(7):1752–1763. doi:10.1007/s11095-009-9886-2
- Khan KA. The concept of dissolution efficiency. *J Pharm Pharmacol*. 1975;27(1):48–49. doi:10.1111/j.2042-7158.1975.tb09378.x
- Duret C, Wauthoz N, Sebti T, Vanderbist F, Amighi K. New inhalation-optimized itraconazole nanoparticle-based dry powders for the treatment of invasive pulmonary aspergillosis. *Int J Nanomedicine*. 2012;7:5475–5489. doi:10.2147/IJN.S34091
- Ishak RA, Osman R. Lecithin/TPGS-based spray-dried self-microemulsifying drug delivery systems: in vitro pulmonary deposition and cytotoxicity. *Int J Pharm*. 2015;485(1–2):249–260. doi:10.1016/j.ijpharm.2015.03.019
- Ungaro F, d'Angelo I, Coletta C, et al. Dry powders based on PLGA nanoparticles for pulmonary delivery of antibiotics: modulation of encapsulation efficiency, release rate and lung deposition pattern by hydrophilic polymers. *J Control Release*. 2012;157(1):149–159. doi:10.1016/j.jconrel.2011.08.010
- Azarmi S, Roa WH, Lobenberg R. Targeted delivery of nanoparticles for the treatment of lung diseases. *Adv Drug Deliv Rev*. 2008;60(8):863–875. doi:10.1016/j.addr.2007.11.006
- Pilcer G, Amighi K. Formulation strategy and use of excipients in pulmonary drug delivery. *Int J Pharm*. 2010;392(1–2):1–19. doi:10.1016/j.ijpharm.2010.03.017
- Al-Qadi S, Grenha A, Carrion-Recio D, Seijo B, Remunan-Lopez C. Microencapsulated chitosan nanoparticles for pulmonary protein delivery: in vivo evaluation of insulin-loaded formulations. *J Control Release*. 2012;157(3):383–390. doi:10.1016/j.jconrel.2011.08.008
- Grenha A, Remunan-Lopez C, Carvalho EL, Seijo B. Microspheres containing lipid/chitosan nanoparticles complexes for pulmonary delivery of therapeutic proteins. *Eur J Pharm Biopharm*. 2008;69(1):83–93. doi:10.1016/j.ejpb.2007.10.017
- Sinsuebpol C, Chatchawalsaisin J, Kulvanich P. Preparation and in vivo absorption evaluation of spray dried powders containing salmon calcitonin loaded chitosan nanoparticles for pulmonary delivery. *Drug Des Devel Ther*. 2013;7:861–873. doi:10.2147/DDDT.S47681
- Gradon L, Sosnowski TR. Formation of particles for dry powder inhalers. *Adv Powder Technol*. 2014;25(1):43–55. doi:10.1016/j.appt.2013.09.012

34. Li X, Vogt FG, Hayes D Jr, Mansour HM. Physicochemical characterization and aerosol dispersion performance of organic solution advanced spray-dried microparticulate/nanoparticulate antibiotic dry powders of tobramycin and azithromycin for pulmonary inhalation aerosol delivery. *Eur J Pharm Sci.* 2014;52:191–205. doi:10.1016/j.ejps.2013.10.016
35. Osman R, Kan PL, Awad G, Mortada N, El-Shamy AE, Alpar O. Spray dried inhalable ciprofloxacin powder with improved aerosolization and antimicrobial activity. *Int J Pharm.* 2013;449(1–2):44–58. doi:10.1016/j.ijpharm.2013.04.009
36. Kumar S, Gokhale R, Burgess DJ. Sugars as bulking agents to prevent nano-crystal aggregation during spray or freeze-drying. *Int J Pharm.* 2014;471(1–2):303–311. doi:10.1016/j.ijpharm.2014.05.060
37. Mehanna MM, Alwattar JK, Elmaradny HA. Optimization, physicochemical characterization and in vivo assessment of spray dried emulsion: A step toward bioavailability augmentation and gastric toxicity minimization. *Int J Pharm.* 2015;496(2):766–779. doi:10.1016/j.ijpharm.2015.11.009
38. Kuehl PJ, Cherrington A, Dobry DE, et al. Biologic comparison of inhaled insulin formulations: exubera and novel spray-dried engineered particles of dextran-10. *AAPS Pharm SciTech.* 2014;15(6):1545–1550. doi:10.1208/s12249-014-0181-0
39. Moghaddam PH, Ramezani V, Esfandi E, et al. Development of a nano-micro carrier system for sustained pulmonary delivery of clarithromycin. *Powder Technol.* 2013;239:478–483. doi:10.1016/j.powtec.2013.02.025
40. Osman R, Al Jamal KT, Kan PL, et al. Inhalable DNase I microparticles engineered with biologically active excipients. *Pulm Pharmacol Ther.* 2013;26(6):700–709. doi:10.1016/j.pupt.2013.07.010
41. Pomázi A, Buttini F, Ambrus R, Colombo P, Szabó-Révész P. Effect of polymers for aerolization properties of mannitol-based microcomposites containing meloxicam. *Eur Polym J.* 2013;49(9):2518–2527. doi:10.1016/j.eurpolymj.2013.03.017
42. Cruz L, Fattal E, Tasso L, et al. Formulation and in vivo evaluation of sodium alendronate spray-dried microparticles intended for lung delivery. *J Control Release.* 2011;152(3):370–375. doi:10.1016/j.jconrel.2011.02.030
43. Al-Hallak MH, Sarfraz MK, Azarmi S, Roa WH, Finlay WH, Lobenberg R. Pulmonary delivery of inhalable nanoparticles: dry powder inhalers. *Ther Deliv.* 2011;2(10):1313–1324.
44. Gervelas C, Serandour AL, Geiger S, et al. Direct lung delivery of a dry powder formulation of DTPA with improved aerosolization properties: effect on lung and systemic decorporation of plutonium. *J Control Release.* 2007;118(1):78–86. doi:10.1016/j.jconrel.2006.11.027
45. Grenha A, Seijo B, Remuñán-López C. Microencapsulated chitosan nanoparticles for lung protein delivery. *Eur J Pharm Sci.* 2005;25(4–5):427–437. doi:10.1016/j.ejps.2005.04.009
46. Sethuraman VV, Hickey AJ. Powder properties and their influence on dry powder inhaler delivery of an antitubercular drug. *AAPS Pharm SciTech.* 2002;3(4):7–16. doi:10.1208/pt030428
47. Pourshahab PS, Gilani K, Moazeni E, Eslahi H, Fazeli MR, Jamalifar H. Preparation and characterization of spray dried inhalable powders containing chitosan nanoparticles for pulmonary delivery of isoniazid. *J Microencapsul.* 2011;28(7):605–613. doi:10.3109/02652048.2011.599437
48. Chew NY, Chan HK. Use of solid corrugated particles to enhance powder aerosol performance. *Pharm Res.* 2001;18(11):1570–1577. doi:10.1023/a:1013082531394
49. Yue PF, Li Y, Wan J, Yang M, Zhu WF, Wang CH. Study on formability of solid nanosuspensions during nanodispersion and solidification: I. Novel role of stabilizer/drug property. *Int J Pharm.* 2013;454(1):269–277. doi:10.1016/j.ijpharm.2013.06.050
50. Wang Y, Kho K, Cheow WS, Hadinoto K. A comparison between spray drying and spray freeze drying for dry powder inhaler formulation of drug-loaded lipid-polymer hybrid nanoparticles. *Int J Pharm.* 2012;424(1–2):98–106. doi:10.1016/j.ijpharm.2011.12.045
51. Crowder T, Hickey A. Powder specific active dispersion for generation of pharmaceutical aerosols. *Int J Pharm.* 2006;327(1–2):65–72. doi:10.1016/j.ijpharm.2006.07.050
52. Nasr M, Awad GA, Mansour S, Taha I, Al Shamy A, Mortada ND. Different modalities of NaCl osmogen in biodegradable microspheres for bone deposition of risedronate sodium by alveolar targeting. *Eur J Pharm Biopharm.* 2011;79(3):601–611. doi:10.1016/j.ejpb.2011.07.010
53. Yang JJ, Liu CY, Quan LH, Liao YH. Preparation and in vitro aerosol performance of spray-dried Shuang-Huang-Lian corrugated particles in carrier-based dry powder inhalers. *AAPS Pharm SciTech.* 2012;13(3):816–825. doi:10.1208/s12249-012-9806-3
54. Chew NY, Tang P, Chan HK, Raper JA. How much particle surface corrugation is sufficient to improve aerosol performance of powders?. *Pharm Res.* 2005;22(1):148–152. doi:10.1007/s11095-004-9020-4
55. El-Gendy N, Aillon KL, Berkland C. Dry powdered aerosols of diatrizoic acid nanoparticle agglomerates as a lung contrast agent. *Int J Pharm.* 2010;391(1–2):305–312. doi:10.1016/j.ijpharm.2010.03.009
56. Peters K, Leitzke S, Diederichs JE, et al. Preparation of a clofazimine nanosuspension for intravenous use and evaluation of its therapeutic efficacy in murine *Mycobacterium avium* infection. *J Antimicrob Chemother.* 2000;45(1):77–83. doi:10.1093/jac/45.1.77
57. Zhao H, Kang XL, Chen XL, et al. Antibacterial activities of amorphous cefuroxime axetil ultrafine particles prepared by high gravity antisolvent precipitation (HGAP). *Pharm Dev Technol.* 2009;14(5):485–491. doi:10.1080/10837450902762991
58. Esfandi E, Ramezani V, Vatanara A, Rouholamini Najafabadi A, Hadipour Moghaddam SP. Clarithromycin dissolution enhancement by preparation of aqueous nanosuspensions using sonoprecipitation technique. *Iran J Pharm Res.* 2014;13(3):809–818.
59. Ambhore NP, Dandagi PM, Gadad AP. Formulation and comparative evaluation of HPMC and water soluble chitosan-based sparfloxacin nanosuspension for ophthalmic delivery. *Drug Deliv Transl Res.* 2016;6(1):48–56. doi:10.1007/s13346-015-0262-y
60. Galli C. Experimental determination of the diffusion boundary layer width of micron and submicron particles. *Int J Pharm.* 2006;313(1–2):114–122. doi:10.1016/j.ijpharm.2006.01.030
61. Müller RH, Peters K. Nanosuspensions for the formulation of poorly soluble drugs: I. Preparation by a size-reduction technique. *Int J Pharm.* 1998;160(2):229–237. doi:10.1016/S0378-5173(97)00311-6
62. Kumar S, Gokhale R, Burgess DJ. Quality by Design approach to spray drying processing of crystalline nanosuspensions. *Int J Pharm.* 2014;464(1–2):4234–4242.
63. Duret C, Wauthoz N, Sebti T, Vanderbist F, Amighi K. New respirable and fast dissolving itraconazole dry powder composition for the treatment of invasive pulmonary aspergillosis. *Pharm Res.* 2012;29(10):2845–2859. doi:10.1007/s11095-012-0779-4
64. Yamasaki K, Kwok PC, Fukushima K, Prud'homme RK, Chan HK. Enhanced dissolution of inhalable cyclosporine nano-matrix particles with mannitol as matrix former. *Int J Pharm.* 2011;420(1):34–42. doi:10.1016/j.ijpharm.2011.08.010
65. Valizadeh H, Nokhodchi A, Qarakhani N, et al. Physicochemical characterization of solid dispersions of indomethacin with PEG 6000, Myrj 52, lactose, sorbitol, dextrin, and Eudragit E100. *Drug Dev Ind Pharm.* 2004;30(3):303–317. doi:10.1081/ddc-120030426
66. Kho K, Hadinoto K. Optimizing aerosolization efficiency of dry-powder aggregates of thermally-sensitive polymeric nanoparticles produced by spray-freeze-drying. *Powder Technol.* 2011;214(1):169–176. doi:10.1016/j.powtec.2011.08.010
67. Weiler C, Egen M, Trunk M, Langguth P. Force control and powder dispersibility of spray dried particles for inhalation. *J Pharm Sci.* 2010;99(1):303–316. doi:10.1002/jps.21849

68. Yu H, Teo J, Chew JW, Hadinoto K. Dry powder inhaler formulation of high-payload antibiotic nanoparticle complex intended for bronchiectasis therapy: spray drying versus spray freeze drying preparation. *Int J Pharm.* 2016;499(1–2):38–46. doi:10.1016/j.ijpharm.2015.12.072
69. Agrawal S, Ashokraj Y, Bharatam PV, Pillai O, Panchagnula R. Solid-state characterization of rifampicin samples and its biopharmaceutical relevance. *Eur J Pharm Sci.* 2004;22(2–3):127–144. doi:10.1016/j.ejps.2004.02.011
70. Krishnaiah D, Sarbatly R, Nithyanandam R. Microencapsulation of *Morinda citrifolia* L. extract by spray-drying. *Chem Eng Res Des.* 2012;90(5):622–632. doi:10.1016/j.cherd.2011.09.003
71. De Souza VB, Thomazini M, Balieiro J, Fávoro-Trindade CS. Effect of spray drying on the physicochemical properties and color stability of the powdered pigment obtained from vinification byproducts of the Bordo grape (*Vitis labrusca*). *Food Bioprod Process.* 2015;93:39–50. doi:10.1016/j.fbp.2013.11.001
72. Bruni G, Berbenni V, Milanese C, et al. Physico-chemical characterization of anhydrous D-mannitol. *J Therm Anal Calorim.* 2009;95(3):871–876. doi:10.1007/s10973-008-9384-5
73. Kaewjan K, Srichana T. Nano spray-dried pyrazinamide-l-leucine dry powders, physical properties and feasibility used as dry powder aerosols. *Pharm Dev Technol.* 2016;21(1):68–75. doi:10.3109/10837450.2014.971373
74. Chuan J, Li Y, Yang L, et al. Enhanced rifampicin delivery to alveolar macrophages by solid lipid nanoparticles. *J Nanopart Res.* 2013;15(5):1–9. doi:10.1007/s11051-013-1634-1
75. Dong S, Hiraniil AA, Colacino KYR, LEE YW, Roman M. Cytotoxicity and cellular uptake of cellulose nanocrystals. *Nano Life.* 2012;02(03):1241006–1241015.
76. Zhang H, Hollis CP, Zhang Q, Li T. Preparation and antitumor study of camptothecin nanocrystals. *Int J Pharm.* 2011;415(1–2):293–300. doi:10.1016/j.ijpharm.2011.05.075
77. Mahmoud KA, Mena JA, Male KB, Hrapovic S, Kamen A, Luong JH. Effect of surface charge on the cellular uptake and cytotoxicity of fluorescent labeled cellulose nanocrystals. *ACS Appl Mater Interfaces.* 2010;2(10):2924–2932. doi:10.1021/am1006222

International Journal of Nanomedicine

Dovepress

Publish your work in this journal

The International Journal of Nanomedicine is an international, peer-reviewed journal focusing on the application of nanotechnology in diagnostics, therapeutics, and drug delivery systems throughout the biomedical field. This journal is indexed on PubMed Central, MedLine, CAS, SciSearch®, Current Contents®/Clinical Medicine,

Journal Citation Reports/Science Edition, EMBase, Scopus and the Elsevier Bibliographic databases. The manuscript management system is completely online and includes a very quick and fair peer-review system, which is all easy to use. Visit <http://www.dovepress.com/testimonials.php> to read real quotes from published authors.

Submit your manuscript here: <https://www.dovepress.com/international-journal-of-nanomedicine-journal>